JOURNAL OF GEOPHYSICAL RESEARCH, VOL. 105, NO. B8, PAGES 19,253–19,272, AUGUST 10, 2000

Thermochronology of the Torlesse accretionary complex, Wellington region, New Zealand

Peter J. J. Kamp

Department of Earth Sciences, University of Waikato, Hamilton, New Zealand

Abstract. The Torlesse Complex comprises several Mesozoic accretionary prism complexes together forming continental basement over large parts of New Zealand. This study focuses on the thermal history of relatively low grade graywacke rocks exposed in a transect in southern North Island that crosses the structural grain of the Torlesse Complex, including its older and younger parts. Zircon fission track (FT) ages for the Late Triassic Rakaia Terrane, which is the most inboard of the accretionary complexes, are partially annealed, some possibly reset, and may indicate early Cretaceous (134 ± 10 Ma) cooling from maximum temperatures (T_{max}), probably related to imbrication of younger complexes of the Pahau Terrane. Numerical modeling of the zircon FT ages and published $^{40}Ar/^{39}Ar$ muscovite and biotite ages for the Rakaia Terrane suggest T_{max} values of 265-310°C and exhumation from depths of 10–12 km. The rocks underlying the Aorangi Range and involving the youngest accretionary complex have experienced much lower T_{max} values of ≤210° and ≥110°C, bracketed by reset apatite FT ages and detrital zircon FT ages. The occurrence of a circa 100 Ma component of zircon FT ages in both the weakly and highly indurated rocks beneath the Aorangi Range, as well as in remnants of an overlying Albian accretionary slope basin (Whatarangi Formation), imply multistorey accretion and incorporation of sediment into the youngest prism. This circa 100 Ma zircon FT age component also places a maximum age on the termination of Mesozoic subduction beneath the New Zealand region. The occurrence of reset apatite FT ages across the whole of the Wellington transect indicates that at least 4 km of exhumation occurred during the late Miocene.

1. Introduction

The Torlesse Complex comprises an extensive area of Triassic to Late Cretaceous continental basement underlying New Zealand (Figure 1). Previous studies of the Torlesse rocks have concluded that the complex formed in an accretionary prism setting at successive convergent plate margins and that it probably includes several distinct terranes [*Andrews et al.*, 1976; *Bradshaw et al.*, 1981; *MacKinnon*, 1983; *Silberling et al.*, 1988; *George*, 1990; *Suneson*, 1993; *Mazengarb and Harris*, 1994; *Mortimer*, 1995]. In its lithological and structural characteristics the Torlesse Complex is similar to other large sandstone-dominated accretionary complexes in the circum-Pacific region, including the Franciscan Complex in California and the Shimanto Belt in Japan.

The sedimentary facies of the Torlesse Complex, which are far more extensive than the related Alpine Schist and Otago Schist with Torlesse protoliths [*Suggate et al.*, 1978; *Mortimer*, 1993], experienced maximum temperatures and pressures of about 250–330°C and 3–4 kbar [*Mortimer et al.*, 1993]. This temperature range lies within the temperature range of the partial annealing zone of fission tracks in zircon and close to the temperature of total annealing, for which measured ages provide direct dates of the start of the subsequent exhumation and cooling history. In younger parts of the Torlesse Complex the rocks have experienced zeolite facies metamorphism only, suggesting that zircon fission track (FT) ages for these rocks will not have been partially annealed (i.e., T_{max} <210°C [*Tagami et al.*, 1996] and detrital zircons should retain source FT ages. These ages, or components within the single grain age distributions, may provide maximum depositional ages in the graywacke successions that are largely unfossiliferous [e.g. *Garver and Brandon*, 1994]. In this paper, zircon and apatite fission track data are reported and modeled for samples obtained from a transect through the Torlesse Complex in the Wellington area of southern North Island. These results, together with previously published $^{40}Ar/^{39}Ar$ ages, are numerically modeled and interpreted to establish the thermal history experienced by the rocks. This provides constraints bearing on current issues surrounding the Torlesse Complex including the timing of basement amalgamation, the age and distribution of terranes within the Torlesse Complex in North Island, the Cretaceous timing of termination of subduction in the New Zealand region, and interpretation of whole rock K-Ar and Rb-Sr data for accretionary rocks.

Paper number 2000JB900163
0148-0227/00/2000JB900163$09.00

2. Tectonic and Geological Setting

On the basis of differences in age, petrography, and bulk chemical composition the Torlesse Complex has been subdivided into three tectonostratigraphic terranes, which have traditionally been called subterranes (Rakaia, Pahau, and Waioeka Terranes) [*Bradshaw et al.*, 1981; *Mortimer*, 1995]. These terranes crop out in the Wellington transect (Figure 2), which lies orthogonal to the regional and mesoscopic structures. Deeper structural levels are exposed in the more inboard and western Triassic Rakaia Terrane compared with the younger terranes to the east [*Begg and Mazengarb*, 1996].

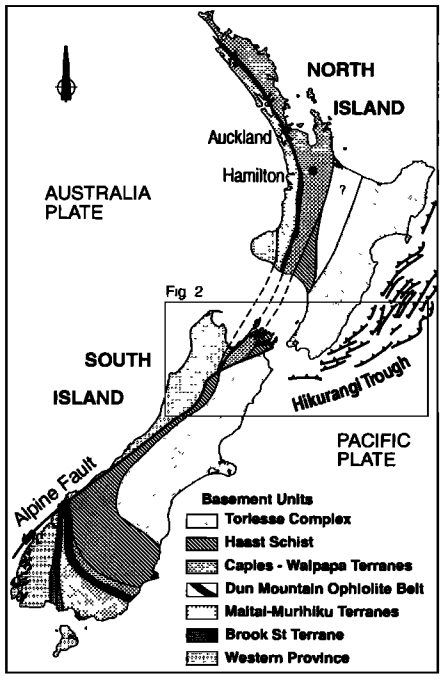

Figure 1. Simplified distribution of the main basement terranes onshore in New Zealand based on several sources including *Coombs et al.* [1996] and *Spörli* [1978]. Note in particular the extent of the Torlesse Complex, which includes several terranes.

2.1. Rakaia Terrane

The Rakaia Terrane (Figure 2), also mapped in southern North Island as the Wellington Belt (Figure 3) [*Begg and Mazengarb*, 1996], typically comprises complexly folded alternating beds of graywacke and argillite. Continuous stratigraphic sequences are rarely more than 100 m thick due to fault imbrication. Basalt, colored argillite, chert, and limestone in various associations are known at several localities [*Reed*, 1957; *Grapes et al.*, 1990]. The sandstone beds are typically fine-grained, poorly sorted feldsarenites with variable lithic proportions. In sandstone beds, matrices are weakly recrystallized with fine sericite-chlorite, rare biotite, ± prehnite and pumpellyite. Zones of semischist up to textural zone IIB occur west of Wellington Fault (Figure 3) and comprise the metamorphic mineral associations quartz + albite + muscovite + chlorite + titanite + pumpellyite ± prehnite ± stilpnomelane, suggestive of a westward increase in metamorphic grade [*Mortimer et al.*, 1993; *Begg and Mazengarb*, 1996]. Maximum temperatures and pressures of about 250–300°C and 3–4 kbar for upper prehnite-pumpellyite facies in Rakaia Terrane sandstone and semischist have been estimated qualitatively by *Mortimer et al.* [1993]. Bedding attitudes are normally steep. Melange and broken formation are widespread components of Rakaia Terrane in the Wellington region, ranging from meters to kilometers in thickness, and are interpreted as decollements where coherent blocks of strata were imbricated by east directed thrusting [*Suneson*, 1993]. The sandstone beds show all degrees of disruption ranging up to boudins and rods. Fossil localities are rare, but different types of fauna recovered (chiefly radiolarians and bivalves including *Halobia* and *Monotis*) indicate a late Triassic (Late Carnian–Rhaetian; 225–205 Ma [*Gradstein et al.*,1994]) depositional age [*Campbell*, 1982; *Blome et al.*, 1987; *Grapes et al.*, 1990; *Grapes and Campbell*, 1994; *Begg and Mazengarb*, 1996]. The radiolarian fossils have been recovered chiefly from phosphorites within argillite beds in alternating sandstone and argillite successions and from widespread localities and are considered to date the enclosing sediments. This is also the case for the bivalves, which are usually enclosed in sandstone.

2.2. Rimutaka Melange

The Rimutaka Melange (Figure 3) is characterized by melange and broken formation that surround sandstone-dominated blocks up to kilometer in size and similar in lithology to the Wellington Belt [*Begg and Mazengarb*, 1996]. Other lithologies in the terrane include basalt, limestone, chert, diamictite, green volcaniclastic argillite, and a basalt dike. The Rimutaka Melange is distinguished from the Wellington Belt by the regional extent of its melange/broken formation. Schistosity is not developed. The metamorphic grade of the Rimutaka Melange appears to be variable: zeolites are absent, prehnite is rare, and the presence of pumpellyite is sporadic, suggesting lower prehnite-pumpellyite facies conditions. However, low conodont color alteration index CAI values of 1 to 1.5, suggestive of maximum temperatures <90°C, have been reported from a limestone block [*Begg and Mazengarb*, 1996].

Depositional ages of the Rimutaka Melange are based chiefly on radiolarians, giving an age range of Middle Jurassic to Early Cretaceous, for localities well north of the coastal outcrops [*Foley et al.*, 1986], and from Late Jurassic (Late Kimmeridgian–Early Tithonian) to possibly Early Cretaceous based on microfossils and macrofossils out of allochthonous limestone blocks [*Begg and Mazengarb*, 1996].

2.3. Aorangi Range, Waioeka Terrane

The basement rocks underlying the Aorangi Range (Figures 2 and 3) comprise very similar lithologies and structural fabrics to those already described for the Rakaia Terrane in the Wellington Belt. For the Aorangi Range these have been described in detail by *George* [1990] and the style of deformation has been interpreted as arising from accretion of thick trench fill into a growing accretionary prism. Metamorphic grade barely reaches zeolite facies in graywacke sandstone of Albian age (Mangapoikia Formation) at the northern end of the Aorangi Range [*Barnes and Korsch*, 1990, 1991]. The metamorphic mineralogy of the more indurated rocks at the southern end of the Aorangi Range is not well established but has been described as low prehnite-pumpellyite grade without lawsonite by *George* [1990]. *Adams and Graham* [1996] noted that to date there has been no clear documentation of pumpellyite east of the Rimutaka Ranges (i.e., in Aorangi Range).

An important structural element of basement in the Aorangi Range is the occurrence of relatively undeformed, mass-emplaced trench-slope basin deposits (Whatarangi Formation) (Figures 2 and 3) of zeolite metamorphic grade above the accreted part of the prism succession [*George*, 1992]. The preservation of these deposits supports the higher structural level and lower metamorphic grade (i.e., zeolite to prehnite) of the underlying accreted rocks compared with those cropping out in the Rakaia Terrane to the west. Macrofossils contained in boulders derived from the Whatarangi Formation yield a small bivalve *Maccoyella* sp implying an age within the Albian-Aptian [*Speden*, 1968]. No macrofossil localities are known from the basement complex in the southern parts of the Aorangi Range, but it has long been assigned a late Jurassic–early Cretaceous age [*Speden*, 1976], leading to classification of them as part of the Pahau Terrane

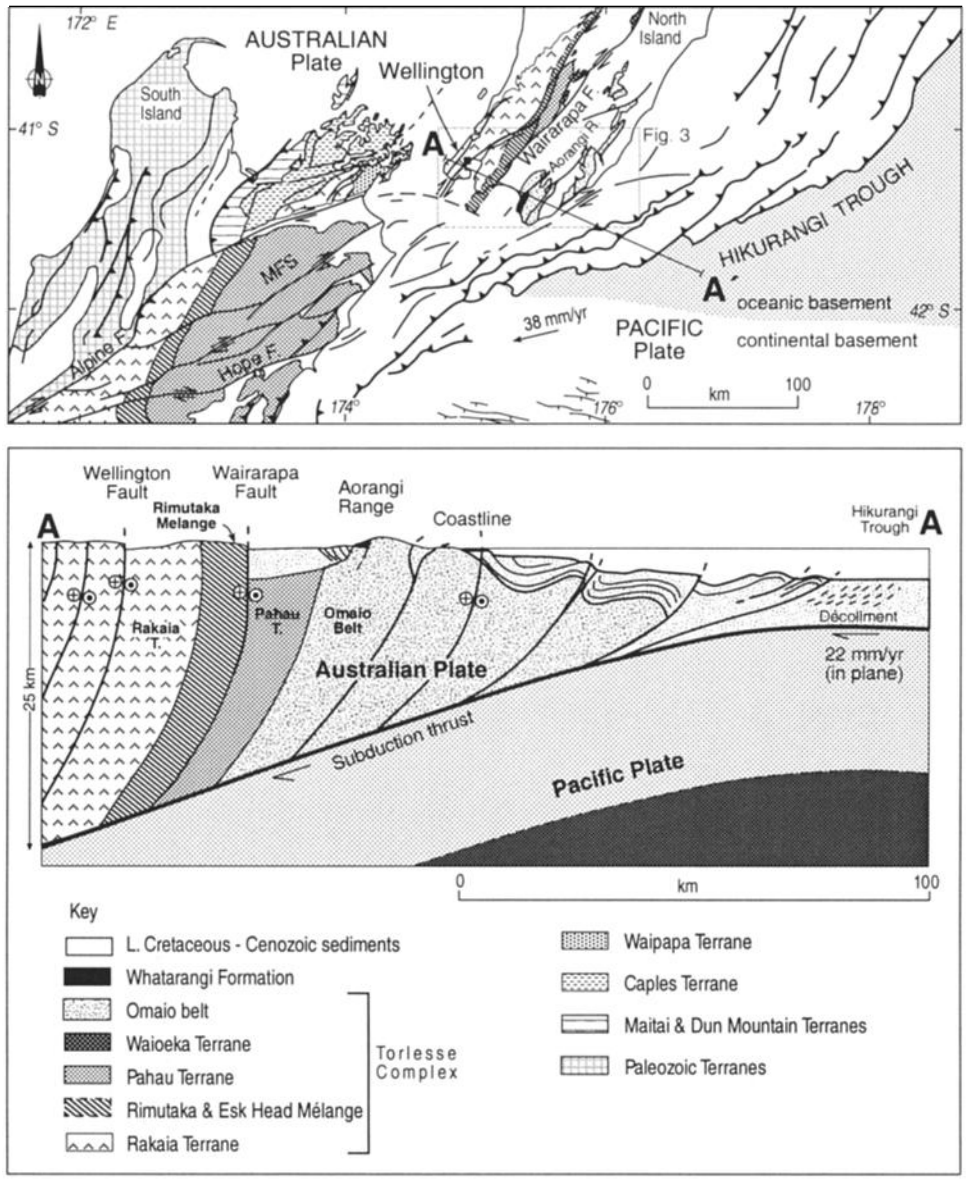

Figure 2. Map of central New Zealand showing the distribution of terranes and other rock units onshore [from *Mortimer* 1993; *Mortimer et al.*, 1997] and the faults offshore [from *Barnes et al.*, 1998]. Cross section shows schematically the distribution of terranes within the Torlesse Complex. MFS is abbreviation for Marlborough Fault System.

[e.g., *George*, 1990]. Well-preserved radiolarians have, however, been recovered from colored argillites associated with metabasite (seamounts) at two localities in the southern part of the range [*George*, 1993]. Overall, the radiolarian assemblage contains forms with long age ranges from the latest Jurassic to Cretaceous, including two species that have ranges extending into the Late Cretaceous. In the Mangatoetoe Stream locality of *George* [1993], the occurrence of *Pseudodictyomitra lodagoensis* Passagno (C. Hollis, written communication, 1998) suggests an Albian-Cenomanian (110–93.5 Ma) range, whereas at Cape Palliser the occurrence of *Stichomitra manifesta* implies a Coniacian to Santonian (89.0–82.0 Ma) age [*Hashimoto and Ishida*, 1997]. The possibility of a Late Cretaceous age for these rocks was discounted by *George* [1993] as reflecting biogeographic provincialism due to the probable (older) Albian-Aptian age range inferred for the overlying Whatarangi Formation. Zircon fission track ages reported here lend support to the Late Cretaceous radiolarian ages and indicate that the rocks are younger than Pahau Terrane rocks in the axial ranges of North Island. This paper develops a case for an extensive area in eastern North Island of mid to late Cretaceous accretionary complexes (Omaio belt).

2.4. Modern Subduction Geometry: Analogue for the Mesozoic

The Torlesse Complex throughout North Island and northernmost South Island currently lies in a forearc setting (Figure 2). The geometry and structure of the modern subduction zone is well constrained beneath the shelf and slope leading down to the Hikurangi Trough by shallow and deep seismic reflection images [*Davey et al.*, 1986; *Barnes et al.*, 1998]. At greater depths beneath the Torlesse Complex the position of the

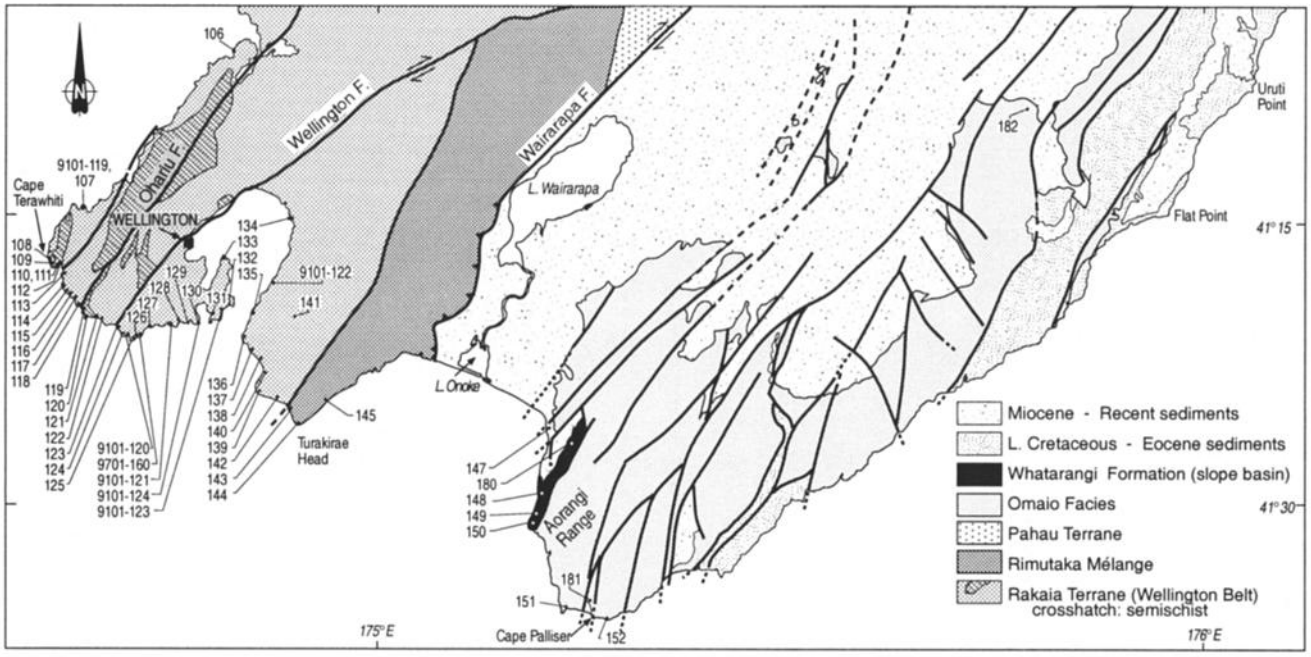

Figure 3. Map of southern North Island showing the sample locations in relation to general geological units. The hatched area in Rakaia Terrane shows the extent of semischist [after *Begg and Mazengarb*, 1996].

subduction interface is mapped from active source seismic experiments and by the depth distribution of microseismicity [*Robinson*, 1978, 1986]. The subduction thrust appears to have a recent history of alternate coupling and uncoupling [*Walcott*, 1978], resulting in structural imbrication during the Late Cenozoic in the same sense as the Mesozoic phase of deformation. The history of relative Australian-Pacific plate motion [*Stock and Molnar*, 1982] suggests that the slab has been beneath the Wellington region for ~5 m.y. During this time a high flux of sediments sourced from erosion of Torlesse rocks in the Southern Alps collision zone has constructed a late Neogene accretionary prism outboard of the youngest Mesozoic accretionary complex (Figure 2). Concurrently, a wedge of post (Mesozoic) subduction, latest Cretaceous-Oligocene fine-grained sediments deposited on top of the Torlesse Complex has been deformed by reverse faulting and subduction kneading and now underlies the shelf and upper slope parts of the late Neogene prism. Hence, during the Miocene-Pleistocene a subduction geometry akin to that existing up to the late Cretaceous has been reestablished. Active oblique-slip faults such as the Wellington and Wairarapa Faults have juxtaposed blocks as a result of kilometers of right-lateral movement (Figure 2), which in turn has been driven by oblique subduction of the Pacific Plate.

3. Fission Track Thermochronology and Detrital FT Thermochronology

Fission track thermochronology relies upon the formation and repair of fission damage (tracks) to the crystallographic structure of uranium bearing minerals such as apatite, zircon, and titanite, arising from the spontaneous fission of 238U [Fleischer et al., 1975]. The basis of fission track analysis as it applies to apatite and zircon, the principles of interpretation of fission track data, and the forward modeling procedures commonly applied to reconstruct thermal histories have been described in a series of papers [Gleadow et al., 1986; Green et al., 1986, 1989; Gallagher, 1995; Gallagher et al., 1998; Tagami et al., 1998]. Examples of applications of the technique to basement provinces include the papers by Hurford [1986], Gleadow and Fitzgerald [1986], and Kamp et al. [1989].

In these conventional types of thermochronological studies, information is obtained about the thermal history experienced by the host rocks, including maximum temperatures achieved, and the timing and style of cooling. Detrital FT thermochronology differs from conventional FT thermochronology in that the distribution of FT grain ages within a sample, particularly for sediments, can arise from crystals originating from a variety of thermotectonic source terrains, unlike a conventional FT age, where all the grains dated from a sample have had a common thermal history. Hence, in detrital FT studies one explores the provenance and age information contained in rocks that have not been partially overprinted since deposition [e.g., Hurford et al., 1984; Garver and Brandon, 1994; Garver et al., 1999]. Both conventional and detrital FT thermochronological approaches have been applied in this study, thereby establishing maximum paleotemperatures in the Rakaia Terrane and in blocks of sandstone in the Rimutaka Melange and constraining depositional ages in the accretionary complex farther east.

3.1. Experimental Procedures

Apatite and zircon concentrates were separated from 2–4 kg samples of sandstone basement from the southern coastline of North Island (Table 1) using standard magnetic and heavy liquid techniques. These concentrates were prepared for irradiation in the nuclear reactor at Oregon State University, following the procedures outlined by *Green* [1985] and *Kamp et al.* [1989]. In particular, the Teflon zircon mounts were etched in NaOH:KOH eutectic solution at 230 ± 1°C for ~25 hours. The external detector method [*Gleadow*, 1981] has been used exclusively throughout this study. The fission track ages were determined using the zeta calibration method [*Hurford and Green*, 1982; *Green*, 1985]. Fission track ages were calculated as central ages

[*Galbraith and Green*, 1991]. Confined track lengths in apatite sample mounts were measured using a digitizing tablet connected to a computer, superimposed on the microscope field of view via a projection tube. This system was calibrated against a stage graticule ruled in 2-μm divisions. Tracks can be measured with a precision ±0.2 μm with this system. Tracks were measured using the recommendations of *Laslett et al.* [1982].

Apatite crystals in six polished grain mounts from Rakaia Terrane, for which density (age) and length measurements were made, were analyzed by electron microprobe at the School of Earth Sciences, University of Melbourne, to determine major element composition. A Cameca SX 50 was used to analyze elements by wavelength dispersive spectroscopy. Operating conditions included 15.0 kV voltage at 2.5 x 10^{-8} A and a counting time of 40 s per element, with chlorine and fluorine measurements being made first.

Table 1. Map Locations (New Zealand Map Series 260 Grid) for Torlesse Complex Samples, Wellington Region

Sample	Easting	Northing
9701 -106	2664000	5909900
-107	2653300	5997300
-108	2645300	5989300
-109	2645500	5988900
-110	2645700	5988700
-111	2645700	5988800
-113	2646700	5988600
-114	2646400	5988000
-115	2646600	5986700
-116	2647100	5986000
-117	2647600	5985600
-118	2648200	5984800
-119	2648600	5984200
-120	2648800	5983700
-121	2649900	5983800
-122	2650500	5983600
-123	2652000	5982700
-124	2652400	5982300
-125	2653600	5981400
-126	2654200	5981900
-127	2655700	5982800
-128	2657900	5982800
-129	2658900	5983000
-130	2659900	5982900
-131	2661500	5983500
-132	2663200	5984500
-133	2662900	5989800
-134	2669500	5993200
-135	2665700	5984200
-136	2664600	5981400
-137	2665700	5979900
-138	2666600	5978900
-139	2666300	5975900
-140	2667400	5977800
-141	2670100	5983900
-142	2667900	5975500
-143	2669600	5974300
-144	2670400	5973100
-145	2673500	5975500
-148	2694500	5966200
-149	2694200	5963700
-150	2693600	5962500
-151	2696700	5953800
-152	2700900	5952400
-160	2654500	5981800
-180	2697300	5970500
-181	2699100	5953500
-182	2744200	6001700
9101 -119	2653400	5997200
-120	2652600	5981900
-121	2656400	5982700
-122	2667800	5987200
-123	2663100	5984400
-124	2659800	5983000

4. Apatite FT Results and Interpretations: Magnitude of Neogene Exhumation

Analytical data for apatite samples are shown in Table 2 and are illustrated in Figures 4 and 5. These data fall into three distinct age groups, two having Neogene ages (Figure 5) and the third comprising one sample (9701-182) obtained from basement west of Flat Point (Figure 3), which has an age of about 78 Ma.

Apatite ages for Rakaia Terrane and Rimutaka Melange rocks range from 5.3 ± 1.2 to 12.7 ± 3.8 Ma, with mean lengths in the range 14.65 ± 0.38 to 16.24 ± 0.34 μm. These late Miocene ages are significantly younger than the Late Triassic or Late Jurassic depositional ages of the host rocks, indicating that they have resided at elevated temperatures where all the tracks were fully annealed prior to late Miocene cooling.

The apatite FT data for this group of 42 samples appears to show no spatial pattern (Figure 4). At the 2σ error level the ages and lengths for all of the samples overlap (Figures 4 and 5). The weighted mean age of the samples is 8.5 ± 0.3 Ma, which is a minimum estimate of when cooling of the samples started.

The chlorine contents of 131 apatite crystals probed from six samples are illustrated in Figure 6. The Rakaia Terrane (Wellington Belt) apatites have predominantly fluorapatite compositions, but in most samples, there are a few crystals that contain reasonably high chlorine contents of up to 1.9 wt %. This variation in composition might be expected to influence the track annealing properties [*Green et al.*, 1986], but in this case where the rocks have cooled rapidly, the effects will be negligible. The average chlorine contents suggest that the apatite FT closure temperature for Durango apatite of 110 ± 10°C probably applies in this study.

The FT thermochronological signal arising from the data for the Wellington Belt appears to be simple. The rocks cooled through 110 ± 10°C at about 8.5 Ma, which was probably achieved by denudation, the amount since then (4 km for a paleogeothermal gradient of 25°C/km) being about the same throughout the Wellington transect. The very long weighted mean track length of 15.3 ± 0.01 μm for the samples indicates that the rate of cooling through the partial annealing zone was very rapid, probably achieved within a couple of million years. This is supported by the occurrence of remnants of late-early Pliocene shelf marine deposits on top of basement in the Wellington region [*Begg and Mazengarb*, 1996]. Because no partially annealed samples have been identified, the timing of cooling given above will be a minimum estimate; erosion could have started earlier, the actual record of its initiation having been removed by the subsequent erosion. A feature of interest is that the late Miocene erosion is not offset significantly by the Wellington and Ohariu Faults. This implies that the geomorphic

Table 2. Apatite Fission Track Data for Torlesse Complex, Wellington

Sample	Number of Crystals	Spontaneous		Induced		$P(\chi^2)$, %	$\rho_s/\rho_i \pm 1\sigma$	ρ_d	N_d	Age ± 1σ, Ma	Mean Track Length ± 1σ, μm	Standard Deviation, μm	Number of Lengths
		ρ_s	N_s	ρ_i	N_i								
9701-108	20	0.075	52	2.728	1903	56.8	-	1.433	3399	6.7 ± 1.0	14.65 ± 0.38	0.38	2
9701-109	20	0.053	16	2.194	658	93.5	-	1.443	3424	6.0 ± 1.5	15.73 ± 0.44	0.88	5
9701-110	20	0.039	17	1.559	688	53.8	-	1.453	3448	6.2 ± 1.5	14.81 ± 0.23	0.65	9
9701-113	10	0.082	12	3.202	471	95.8	-	1.483	3519	6.5 ± 1.9	-	-	-
9701-114	20	0.115	65	2.692	1525	48.4	-	1.477	3504	10.8 ± 1.4	16.24 ± 0.34	1.02	10
9701-115	20	0.056	27	2.183	1046	71.6	-	1.470	3488	6.5 ± 1.3	15.20 ± 0.19	1.08	34
9701-116	20	0.034	20	1.621	957	6.1	-	1.464	3473	5.3 ± 1.2	15.14 ± 0.12	0.89	51
9701-117	20	0.193	102	4.689	2483	36.0	-	1.458	3458	10.3 ± 1.1	16.00 ± 0.56	1.48	8
9701-118	6	0.046	3	1.909	125	12.8	-	1.451	3442	6.0 ± 3.5	15.46 ± 0.31	0.31	2
9701-119	20	0.078	36	3.444	1595	58.2	-	1.444	3427	5.6 ± 1.0	14.89 ± 0.22	0.87	17
9701-120	8	0.085	7	2.229	184	90.9	-	1.431	3396	9.3 ± 3.6	-	-	-
9701-121	20	0.171	74	3.443	1493	74.0	-	1.425	3381	12.1 ± 1.5	15.22 ± 0.19	0.94	25
9701-122	20	0.121	45	2.806	1044	<0.1	0.045 ± 0.017	1.412	3350	10.9 ± 3.3	15.56 ± 0.28	0.55	5
9701-123	20	0.091	23	2.392	606	97.3	-	1.406	3335	9.2 ± 2.0	15.41 ± 0.32	0.78	7
9701-124	20	0.137	49	2.834	1014	12.9	-	1.399	3319	11.6 ± 1.7	15.25 ± 0.25	0.90	14
9701-125	20	0.057	15	2.407	635	3.4	0.065 ± 0.050	1.393	3304	5.6 ± 1.5	15.75 ± 0.32	0.56	4
9701-126	9	0.045	6	1.801	241	29.7	-	1.386	3289	5.9 ± 2.5	-	-	-
9701-127	20	0.179	52	3.522	1026	0.1	0.049 ± 0.016	1.380	3273	11.8 ± 2.9	14.98 ± 0.21	0.86	18
9701-128	20	0.109	36	3.007	996	99.2	-	1.373	3258	8.5 ± 1.5	15.47 ± 0.20	0.89	20
9701-129	20	0.151	67	4.071	1804	83.1	-	1.360	3242	8.7 ± 1.1	15.43 ± 0.36	1.18	12
9701-130	20	0.088	22	2.043	508	97.7	-	1.315	3120	9.8 ± 2.1	15.32 ± 0.19	1.01	29
9701-131	19	0.097	44	2.178	988	86.6	-	1.324	3141	10.1 ± 1.6	15.74 ± 0.31	0.69	6
9701-132	20	0.057	19	1.823	609	97.7	-	1.333	3162	7.1 ± 1.7	16.24 ±	-	1
9701-133	20	0.122	40	2.982	982	95.2	-	1.341	3182	9.4 ± 1.5	-	-	-
9701-134	20	0.102	63	2.725	1686	89.7	-	1.359	3224	8.7 ± 1.1	15.66 ± 0.10	0.82	68
9701-135	20	0.106	61	2.456	1408	75.9	-	1.368	3245	10.2 ± 1.3	15.55 ± 0.23	0.79	13
9701-136	20	0.070	16	1.640	375	93.4	-	1.377	3266	10.1 ± 2.6	15.35 ± 0.34	0.83	7
9701-137	20	0.148	48	3.136	1015	99.7	-	1.385	3386	11.2 ± 1.7	15.39 ± 0.21	0.67	11
9701-138	20	0.110	35	2.688	857	79.9	-	1.394	3307	9.8 ± 1.7	14.83 ± 0.24	0.77	11
9701-139	20	0.101	44	2.405	1050	64.7	-	1.403	3328	10.1 ± 1.6	14.86 ± 0.17	0.59	13
9701-140	20	0.134	27	3.126	629	95.5	-	1.411	3349	10.4 ± 2.1	15.24 ± 0.17	0.78	23
9701-141	7	0.054	5	1.624	151	64.1	-	1.420	3370	8.1 ± 3.7	-	-	-

Table 2. (continued)

Sample	Number of Crystals	Spontaneous ρ_S	Spontaneous N_S	Induced ρ_i	Induced N_i	$P(\chi^2)$, %	$\rho_s/\rho_i \pm 1\sigma$	ρ_d	N_d	Age ± 1σ, Ma	Mean Track Length ± 1σ, μm	Standard Deviation, μm	Number of Lengths
9701-142	20	0.068	23	1.682	573	82.3	-	1.438	3411	9.9 ± 2.1	15.00 ± 0.29	0.71	7
9701-143	20	0.083	28	2.190	740	19.8	-	1.447	3432	9.4 ± 1.8	14.74 ± 0.26	0.45	4
9701-144	20	0.107	45	2.798	1179	97.5	-	1.455	3453	9.5 ± 1.5	15.20 ± 0.28	0.90	11
9701-145	20	0.074	32	2.096	909	98.3	-	1.464	3474	8.8 ± 1.6	14.97 ±	-	1
9701-148	10	0.197	63	2.314	740	53.3	-	1.353	3210	19.8 ± 2.6	15.03 ± 0.93	1.86	5
9701-149	20	0.117	42	1.683	602	96.3	-	1.359	3224	16.3 ± 2.6	14.15 ± 0.33	0.57	4
9701-150	20	0.157	83	1.634	867	94.5	-	1.365	3239	22.4 ± 2.6	14.73 ± 0.39	1.04	8
9701-151	15	0.122	29	1.812	430	94.0	-	1.372	3254	15.9 ± 3.1	15.50 ± 0.31	0.61	5
9701-160	5	0.151	10	4.049	269	81.4	-	1.409	3342	9.0 ± 2.9	14.31 ±	-	1
9101-119	5	0.138	12	2.241	195	75.6	-	1.205	5961	12.7 ± 3.8	-	-	-
9101-120	10	0.047	11	1.677	393	96.5	-	1.205	5961	5.8 ± 1.8	-	-	-
9101-121	20	0.097	54	2.414	1344	49.1	-	1.205	5961	8.3 ± 1.2	15.45 ± 0.31	0.93	10
9101-122	20	0.136	65	2.778	1330	0.1	0.060 ± 0.029	1.205	5961	11.1 ± 3.5	15.07 ± 0.27	0.66	7
9101-123	10	0.088	11	2.303	287	69.1	-	1.205	5961	7.9 ± 2.4	-	-	-
9701-180	20	0.196	24	4.157	722	99.9	-	1.878	4455	15.4 ± 2.7	14.72 ± 0.30	0.84	8
9701-181	20	0.189	62	3.662	1199	98.4	-	1.888	4479	17.0 ± 2.2	13.27 ± 0.15	1.3	80
9701-182	46	0.680	242	2.855	1016	99.6	-	1.899	4503	78.4 ± 5.9	14.16 ± 0.34	1.24	13

Track densities (ρ) are x 10^6 tracks cm^{-2}. All analyses are by the external detector method using 0.5 for the $4\pi/2\pi$ geometry correction factor. Apatite ages are calculated using dosimeter glass SRM 612 and zeta-612 = 343.5 ± 4.5 (± 1σ). $P(\chi^2)$ is the probability of obtaining χ^2 value for ν degrees of freedom (where ν is the number of crystals -1) [*Galbraith*, 1981]; pooled ρ_s/ρ_i ratio is used to calculate age and uncertainty where $P(\chi^2)$ >5%; mean ρs/ρi ratio is reported for samples where $P(\chi^2)$ <5% and for which central ages [*Galbraith and Green*, 1991] are calculated.

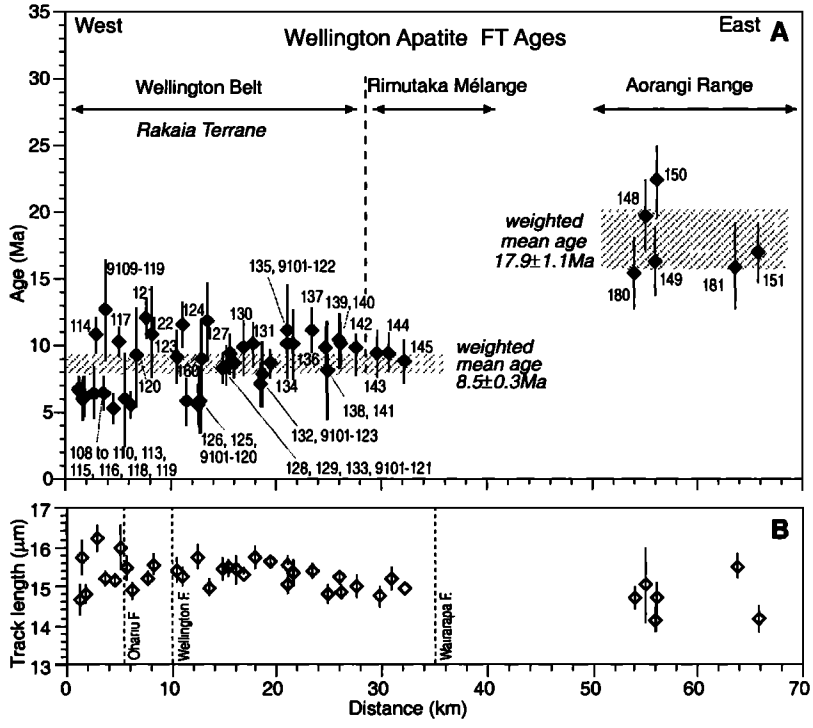

Figure 4. (a) Apatite fission track age versus distance eastward along the transect (Figure 2), and (b) fission track length versus distance. All the apatite ages are reset.

offsets observed in the modern landscape may be close to the actual Quaternary strain.

Apatite FT data have also been obtained for Mesozoic rocks along the southern margin of the Aorangi Range (Figure 3). The six ages overlap at the 2σ error level and have a weighted mean age of 17.9 ± 1.1 Ma (Figure 4). The mean track lengths have some variability (Figures 4 and 5), averaging 14.69 ± 0.23 μm. The track lengths indicate, nevertheless, that the observed ages are reset, being minimum ages of the timing of initiation of cooling. In addition, at least 4 km of denudation, assuming a paleogeothermal gradient of 25°C/km, occurred rapidly during the late early to middle Miocene. Regional stratigraphy brackets the denudation to have occurred between the latest Oligocene and the late Miocene. Remnants of late Miocene (Tongaporutuan Stage, 11.3–6.6 Ma) shelf marine sediments overlie basement in the vicinity of the sample sites. Along the southern North Island transect therefore at least 4 km of the total amount of exhumation of the Torlesse Complex has occurred during the Neogene.

North of the Aorangi Range, apatite FT data were derived for one sample (9701-182) from Albian rocks (Mangapokia Group, Taipo Sandstone [*Moore and Speden*, 1984]) regarded as basement and showing structures indicative of deformation within an accretionary prism. This sample yields an apatite FT age of 78.4 ± 5.9 Ma, with a mean length of 13.27 ± 0.15 μm. Forward modeling of the FT data using monte trax software [*Gallagher*, 1995], and assuming the grains were deposited

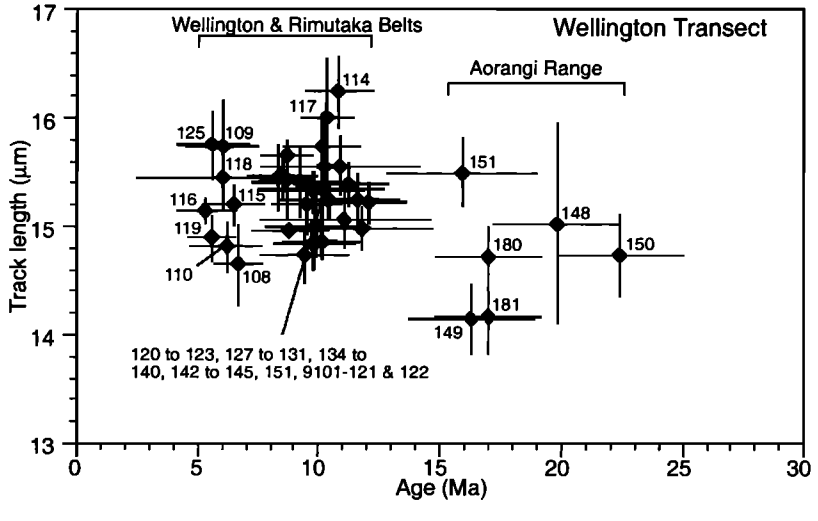

Figure 5. Fission track length versus fission track age for apatite samples from the Wellington transect.

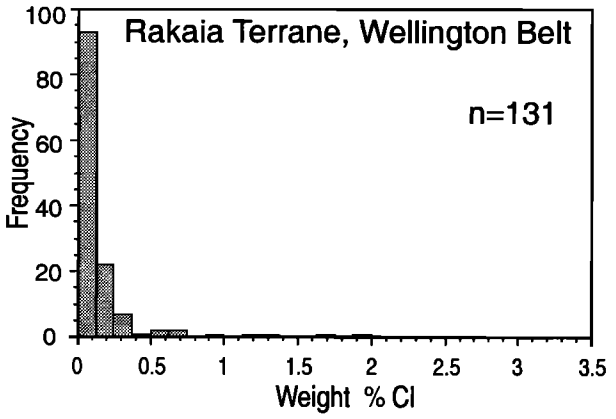

Figure 6. Histogram showing chlorine contents (wt %) of apatite grains for six samples from the Rakaia Terrane in the Wellington Belt.

during the late Albian with no inherited track density, suggests a maximum temperature during the early Miocene of 65–70°C (Figure 7). This amounts to 2.2–2.4 km of Neogene exhumation. The thermal history for the Taipo Sandstone implies that it was accreted into the Cretaceous prism at a very much higher structural level than the basement in the Aorangi Range, a point returned to in section 7.1.

5. Zircon FT and $^{40}Ar/^{39}Ar$ Thermochronology of Rakaia Terrane and Rimutaka Melange

5.1. Zircon FT Results and Interpretations

The zircon FT ages for the Rakaia Terrane fall within the range 143 ± 25 to 232 ± 47 Ma (Table 3). The sample mean ages and their errors are illustrated in Figure 8 for a transect along the southern coastline. All of the samples pass the chi-square test, except for 9701-127. This sample contains one grain that is much older (570 ± 70 Ma) than the others in the sample. The weighted mean age for the 35 Rakaia Terrane samples is 179.9 ± 3.1 Ma. This age and most of the individual sample ages are less than the depositional ages of the host sandstone beds judged from their autochthonous fossil content as described in section 2.1 (Late Carnian-Rhaetian; 225–205 Ma) (Figure 8). This indicates that the succession has been exposed in the past to temperatures sufficient to cause partial annealing of fission tracks in zircon.

Details of the FT ages suggest that the data describe one fossil partial annealing zone. Figure 9 shows all of the single grain ages measured across the 35 zircon FT samples, excluding the 570 ± 70 Ma crystal, on a radial plot in Figure 9a and as a probability density histogram with smoothed curve in Figure 9b. The single grain age data in the two types of plots show a unimodal distribution suggestive of one phase of partial annealing. The spread in the data probably results from the combination of data from samples that experienced slightly different temperature maxima within the partial annealing zone, as well as variable sensitivity of different zircon crystals to annealing arising from different levels of alpha damage together with subtle compositional differences. There is not a marked variation in the sample mean ages along the transect within the Rakaia Terrane and Rimutaka Melange indicative of more highly partially annealed ages in either western or eastern directions (Figure 8). These data support inclusion of the sandstone units within the Rimutaka Melange as originating from Rakaia Terrane and location of the Rakaia-Pahau boundary east of sample site 9701-145, as suggest by *Roser et al.* [1996].

A maximum estimate of the timing of fossilization of the partial annealing that affected the Rakaia Terrane and Rimutaka Melange zircons analyzed can be made from the youngest zircon FT ages. The youngest sample mean ages are around 143–148 Ma for samples 9701–109, 9701-111 and 9701–140 (Table 3). A proportion of the single grain ages are less than this age range, ranging down to about 105 Ma, but with associated errors of 15 m.y. or more. To establish a more robust maximum cooling age estimate, the single grain ages were analyzed using age component analysis software (Fatmix) made available by K. Gallagher, which follows the mathematical principles outlined by *Sambridge and Compston* [1994]. Although the ages have a unimodal distribution (Figure 8), two, three and four components were prescribed in successive analyses of the data to force calculation of a component age incorporating the youngest grains in the distribution. A young mode around 134 ± 10 Ma (three components, 1σ error) or 131 ± 18 Ma (four components, 1σ error) emerges from this analysis. Figure 9 shows the proportion of the data points that would be incorporated in a 134 ± 20 Ma (2σ) mode. A few of the youngest grains lie outside this 2σ error envelope, but this would be anticipated statistically. An age of 134 ± 10 Ma (1σ) is 10 m.y. or so less than the youngest sample mean age and may be a more reasonable maximum estimate for the start of cooling than the age range (143–148 Ma) of the youngest sample mean ages. Alternatively, none of the zircon grains have reset FT ages, and the timing of cooling is later than 134 ± 10 Ma.

5.2. The $^{40}Ar/^{39}Ar$ Ages of Rakaia Terrane

Muscovite and biotite single grain $^{40}Ar/^{39}Ar$ ages have been reported by *Adams and Kelley* [1998] for three Rakaia Terrane

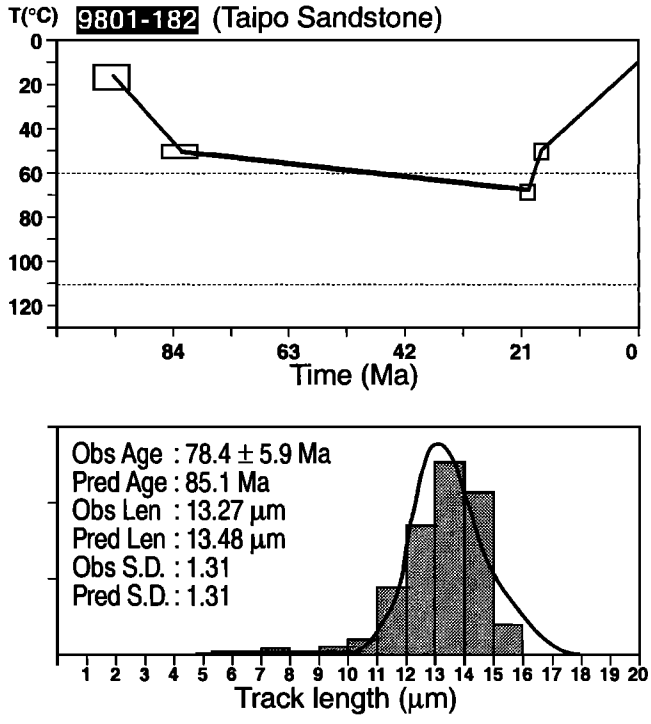

Figure 7. Modeled thermal history for sample 9801-182 from Taipo Sandstone (Mangapokia Group). The T-t history is the average thermal history and the associated uncertainty.

Table 3. Zircon Fission Track Data for Torlesse Complex, Wellington

Sample	Number of Crystals	Spontaneous ρ_s	Spontaneous N_s	Induced ρ_i	Induced N_i	$P(\chi^2)$, %	ρ_s/ρ_i ±1σ	ρ_d	N_d	Age ±1σ, Ma
9701-106	20	9.298	1553	2.610	436	99.5	-	0.830	1973	197.1 ± 12.3
9701-107	20	9.829	1138	3.299	382	92.2	-	0.835	1981	165.9 ± 11.0
9701-109	10	8.968	383	3.395	145	43.1	-	0.842	1998	148.5 ± 15.2
9701-111	5	9.565	118	3.810	47	87.0	-	0.853	2024	143.1 ± 25.1
9701-113	20	10.750	1755	3.253	531	89.4	-	0.861	2042	189.4 ± 11.0
9701-114	20	9.828	886	3.383	305	88.6	-	0.864	2050	167.3 ± 12.2
9701-115	9	11.620	838	3.854	278	91.2	-	0.868	2059	174.4 ± 13.2
9701-117	10	13.920	1281	4.313	397	55.9	-	0.875	2076	188.0 ± 12.2
9701-118	15	11.570	604	3.468	181	68.5	-	0.879	2085	195.2 ± 17.6
9701-120	14	9.169	670	2.751	201	86.9	-	0.889	2110	197.1 ± 16.9
9701-121	11	11.470	729	4.388	279	28.5	-	0.897	2128	156.4 ± 12.0
9701-122	15	9.343	1126	3.203	386	62.0	-	0.900	2136	174.9 ± 11.6
9701-123	15	13.530	1040	3.812	293	69.4	-	0.908	2154	214.1 ± 15.5
9701-124	9	8.634	254	2.753	81	88.8	-	0.911	2162	190.1 ± 24.9
9701-125	12	11.120	538	3.554	172	99.5	-	0.915	2171	190.5 ± 17.6
9701-126	12	9.968	927	3.011	280	47.1	-	0.919	2180	202.3 ± 15.1
9701-127	6	16.860	992	2.668	157	<0.1	4.358 ± 1.099	0.922	2188	232.4 ± 47.3
9701-128	7	8.205	475	2.747	159	62.8	-	0.926	2197	184.2 ± 17.7
9701-129	4	9.233	184	2.910	58	33.3	-	0.929	2205	196.1 ± 30.1
9701-130	20	8.388	1003	2.643	316	49.6	-	0.937	2223	197.8 ± 14.0
9701-133	15	13.300	1704	3.864	495	9.5	-	0.948	2249	216.8 ± 12.8
9701-134	7	11.330	656	3.524	204	20.6	-	0.951	2257	203.3 ± 17.4
9701-136	10	10.230	767	3.615	271	63.4	-	0.958	2274	180.6 ± 13.8
9701-137	12	10.490	866	3.464	286	72.2	-	0.962	2283	193.8 ± 14.4
9701-138	8	12.160	1477	4.050	492	44.3	-	0.966	2292	193.0 ± 11.5
9701-139	14	9.446	1264	3.647	488	61.5	-	0.969	2300	167.4 ± 10.2
9701-140	8	10.390	434	4.622	193	43.8	-	0.973	2309	146.1 ± 13.4
9701-141	11	11.720	1546	3.874	511	13.5	-	0.977	2318	196.6 ± 11.6
9701-142	7	12.44	614	4.296	212	22.8	-	0.980	2326	188.9 ± 16.0
9701-143	5	10.200	271	3.763	100	94.5	-	0.984	2335	177.7 ± 21.4
9701-144	10	10.190	957	3.257	306	81.5	-	0.988	2343	205.4 ± 14.8
9701-145	4	15.520	648	4.838	202	48.2	-	0.991	2352	211.2 ± 18.1
9701-147	4	9.747	296	3.030	92	94.6	-	0.701	1664	150.6 ± 18.6
9701-148	7	5.318	1080	1.659	337	11.6	-	0.706	1675	151.1 ± 10.6
9701-149	3	8.430	144	3.220	55	97.0	-	0.711	1686	124.5 ± 20.1
9701-151	40	9.450	2825	4.426	1323	0.3	2.258 ± 0.128	0.720	1708	101.3 ± 5.7
9701-152	20	9.132	1742	4.047	772	16.0	-	0.725	1720	109.6 ± 5.9
9101-119	7	11.939	921	5.082	392	82.8	-	1.034	2556	162.0 ± 10.8
9101-120	7	11.854	551	5.464	254	55.3	-	1.042	2576	150.9 ± 12.2
9101-121	8	12.541	831	5.207	345	31.6	-	1.050	2596	168.6 ± 11.8
9101-122	7	15.149	366	6.381	366	29.8	-	1.170	2892	185.0 ± 12.6
9101-123	7	13.751	408	6.168	183	96.5	-	1.175	2906	174.6 ± 16.3
9101-124	10	9.586	730	4.465	310	97.3	-	1.181	2920	169.0 ± 12.1

Track densities (ρ) are x 10^6 tracks cm^{-2}. All analyses are by the external detector method using 0.5 for the $4\pi/2\pi$ geometry correction factor. Zircon ages are calculated using dosimeter glass CN1 and zeta-CN1 = 135.1 ± 2.8 (± 1σ) . $P(\chi^2)$ is the probability of obtaining χ^2 value for ν degrees of freedom (where ν is the number of crystals -1) [*Galbraith,* 1981]; pooled ρs/ρi ratio is used to calculate age and uncertainty where $P(\chi^2)$ >5%; mean ρs/ρi ratio is reported for samples where $P(\chi^2)$ <5% and for which central ages [*Galbraith and Green,* 1991] are calculated.

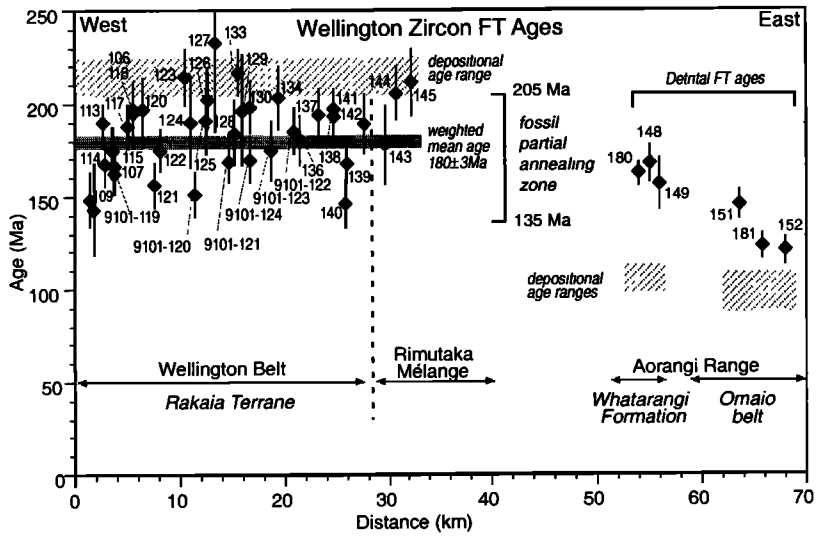

Figure 8. Zircon fission track age versus distance eastward along the Wellington Transect (Figure 2). Ages in the Rakaia Terrane and Rimutaka Melange are partially annealed; those in the Whatarangi Formation and Waioeka Terrane are unannealed in situ and retain source characteristics. Sample 9801-182 is not plotted. The depositional age range shown for the Whatarangi Formation is that implied by *Speden* [1968] based on the occurrence and inferred age of *Maccoyella* sp., which seems to be marginally older than the youngest zircon FT detrital ages obtained for this unit.

sandstone beds from the Wellington region. These combined data are illustrated on radial plots (Figure 10). The muscovite data appear to be described well by four distinct components, for each of which, age and error estimates have been derived by application of K. Gallagher's Fatmix software. There appear to be only two age components in the lesser number of biotite analyses of *Adams and Kelley* [1998] (Figure 10).

The three older age components in the muscovite data are greater than the depositional age of the host rocks and reflect, in part, their provenance. The youngest component (197 ± 2 Ma), however, is marginally less than the youngest possible stratigraphic age of the host rocks. This implies partial argon loss and an element of $^{40}Ar/^{39}Ar$ open system behavior for muscovite during the thermal maximum of the Torlesse Complex. The reduction of at least a few million years of "age" from the grains within the youngest age component due to the loss of the radiogenic daughter product suggests that the other age components will also have lost age, but the amounts cannot be estimated. One of the modes in the biotite data (151.3 ± 12.1 Ma) is also clearly less than the stratigraphic age, which is also attributed here to open system behavior during the thermal maxima in the Torlesse Complex. The observed $^{40}Ar/^{39}Ar$ age reduction is clearer in radial plots (Figure 10) than the histograms as illustrated by *Adams and Kelley* [1998], and its occurrence needs to be considered in evaluation of age matches with possible source areas of sediments in the Rakaia Terrane. An alternative interpretation of the muscovite grain ages is that even the youngest mode (197 ± 2 Ma) reflects provenance age (cooling in the source area) and the rocks accumulated during the Jurassic, meaning that the fossil ages assigned to the rocks are too old.

5.3. Paleotemperature Modeling

Forward modeling of the zircon FT and $^{40}Ar/^{39}Ar$ age reduction has been undertaken using Monte Trax (1998 version) and MacArgon (version 5.12) [*Lister and Baldwin*, 1996] software to estimate the peak temperatures experienced by the Rakaia Terrane in the Wellington Belt. The approach taken follows that of *Baldwin and Lister* [1998], in which numerical models were run with the two software products for a family of possible time-temperature histories differing only in the ambient maximum temperatures possibly experienced by the host rocks during the Jurassic (Figure 11a). The diffusion parameters used for forward modeling of the muscovite and biotite age data are listed in the caption to Figure 11, together with information about the zircon model used. From the 10 different runs of the possible time-temperature histories, curves of modeled age reduction with increasing temperature for each of the three thermochronometers were constructed (Figure 11b). It was then a simple matter to apply the observed FT and $^{40}Ar/^{39}Ar$ ages to those curves to derive the effective maximum temperatures probably experienced by the rocks (Figure 11c).

The curves of modeled age reduction (Figure 11b) are specific to the input time-temperature histories (Figure 11a). It was assumed in the modeling that the muscovite, biotite, and zircon grains started to accumulate radiogenic daughter products (i.e., age) instantaneously at 230 Ma, giving them possibly as little as 5 m.y. of inherited age. It was also assumed that maximum temperatures were reached soon after burial at 200 Ma, consistent with an accretionary prism setting. The first phase of cooling was taken as starting at 135 Ma, which is supported by the youngest zircon FT ages. The rest of the input time-temperature history is constrained by the regional stratigraphy and by apatite FT data but has minimal affect on the model results. The age reduction curves and paleotemperature results are mainly sensitive to the maximum temperature experienced and their duration.

The youngest muscovite $^{40}Ar/^{39}Ar$ age component (197.2 ± 2.4 Ma) implies a maximum temperature in the range 295–305°C (2σ error) (Figure 11c). For the younger biotite age component (151.3 ± 12.1 Ma), it is 290–310°C (2σ error). The weighed mean zircon FT age of 179.9 ± 3.1 Ma implies a maximum temperature between 265° and 282°C. As identified earlier, the range of zircon ages may partly reflect variations in the maximum temperatures experienced by host rocks at different sites. If the fission tracks in the zircon crystals with 134 ± 10 Ma (1σ) ages are genuinely reset, then maximum paleotemperatures of 312–335°C may have been reached by rocks at some sites.

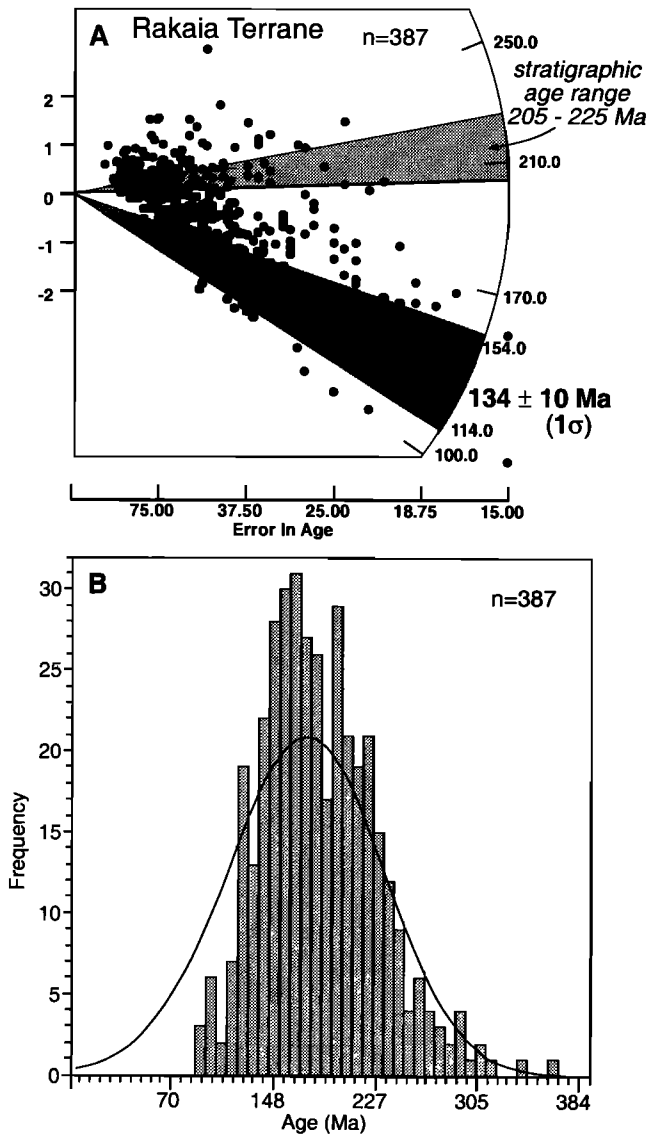

Figure 9. (a) Radial plot showing the distribution of single crystal zircon FT ages for samples from the Rakaia Terrane in the Wellington Belt, and (b) the probability density function (curve) for the same data. See text for discussion.

Alternatively, the kinetic model of track annealing in zircon [*Tagami et al.*, 1998] used to calculate the curve of modeled zircon FT age reduction (Figure 11b), overestimates the temperature at geological timescales of total annealing, which could lead to an overestimation of the maximum temperatures experienced by the Rakaia rocks with reset zircon grains. A review of earlier studies of zircon FT annealing suggests that fission tracks may be close to being totally annealed at 280°C [*Brandon et al.*, 1998]. Taken together, the modeling of three thermochronological systems suggest maximum temperatures within the range 265–310°C were reached by different rocks in the Rakaia Terrane.

6. Detrital FT Thermochronology of the Omaio Belt, Aorangi Range

The sample mean zircon FT ages of rocks from the Aorangi Range lie in the range 156 ± 15 Ma to 120 ± 20 Ma and are older than the corresponding stratigraphic ages based on radiolarian content (Table 3 and Figure 8). They chiefly reflect a provenance signal, although two samples adjacent to dikes show evidence of partial thermal overprinting. Four of the samples originate from rocks regarded as basement, three from the vicinity of Cape Palliser (9701-151, 9701-152, 9701-181), and one from the lower

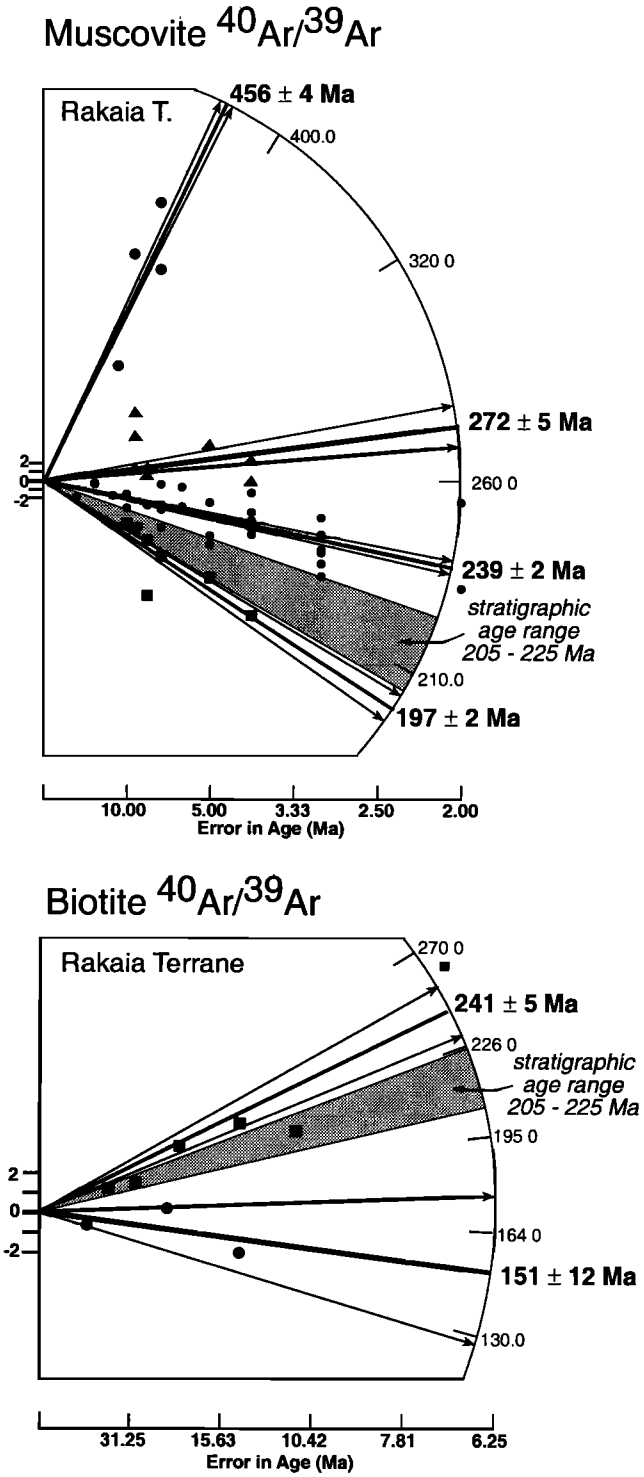

Figure 10. Radial plots of the single-crystal $^{40}Ar/^{39}Ar$ ages reported for muscovite and biotite from Rakaia Terrane (Wellington Belt) by *Adams and Kelley* [1998]. Note that the muscovite data appear to contain four age components and the biotite data appear to contain two components.

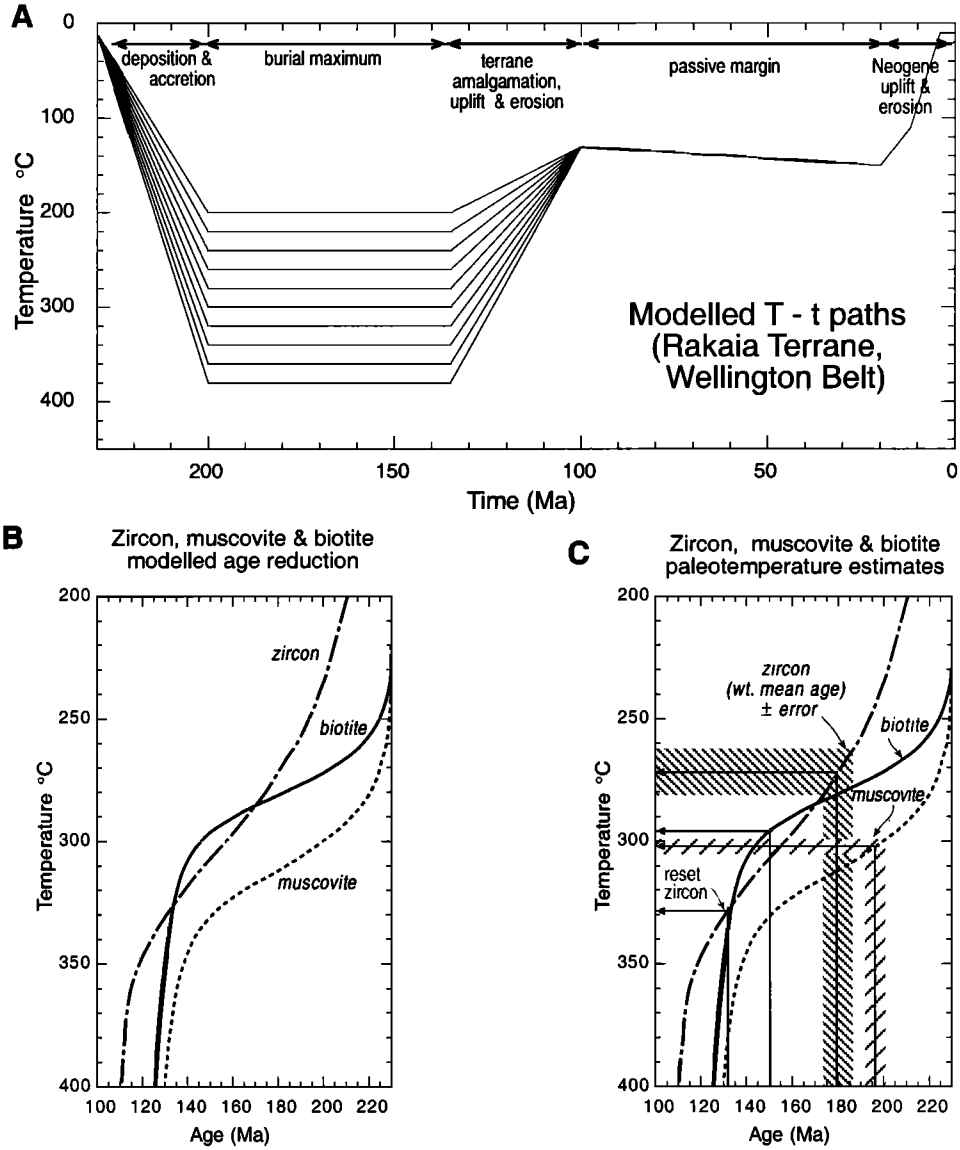

Figure 11. (a) A family of possible T-t histories experienced by the Rakaia Terrane (Wellington Belt) and (b) the resulting $^{40}Ar/^{39}Ar$ muscovite and biotite and zircon fission track apparent age reduction with increasing ambient maximum temperature, based on MacArgon numerical models [*Lister and Baldwin*, 1996] and monte trax (zircon) numerical models [*Gallagher*, 1995]. (c) The probable maximum temperatures experienced by the Rakaia rocks inferred from the age of the youngest muscovite and biotite components in the *Adams and Kelley* [1998] data (Figure 10) and from the weighted mean zircon age for the Rakaia Terrane samples and from the possible reset age (134 ± 10 Ma) of the zircons with the youngest ages. See text for discussion. Diffusion parameters for muscovite are activation energy 41.80 kcal/mol; frequency factor 3.3520 x 10^{-7} cm^2/s; activation volume 10.00 cm^3; radius of diffusion domain 5.90 μm; type of domain slab. For biotite the respective diffusion parameters are 47.00 kcal/mol; 7.7000 x 10^{-2} cm^2/s; 14.00 cm^3; 150.00 μm; cylinder. In forward modeling of the zircon age data the fanning Arrhenius model of *Tagami et al.* [1998] was used.

rank Mangapokia Group (Taipo Sandstone) to the north (9701-182) (Figure 3). Another three samples (9701-148, 9701-149, 9701-180) originate from the Whatarangi Formation, an infaulted remnant of an Albian accretionary slope basin fill. The main signal in the data presented here is that the very low rank basement (Taipo Sandstone), together with the more indurated basement around Cape Palliser, as well as the Whatarangi Formation, all contain a component of zircon crystals with circa 100 Ma detrital ages that may have been accreted more-or-less simultaneously into different levels of the one accretionary prism.

Sample 9701-151 is from sandstone at Cape Palliser headland, juxtaposed with the Cape Palliser volcanic sequence of pillowed metabasite, considered to be remnants of a dismembered seamount accreted to the overlying plate [*George*, 1993]. The 50 grains dated in this sample failed the chi-square test. Age component analysis, in which two components are prescribed, give ages of 163 ± 9 Ma and 99 ± 5 Ma (Figure 12a); for three components the ages are 204 ± 17, 135 ± 11, and 91 ± 8 Ma, but this may overinterpret the number of modes. The ages of the young mode in both analyses overlap however. The more

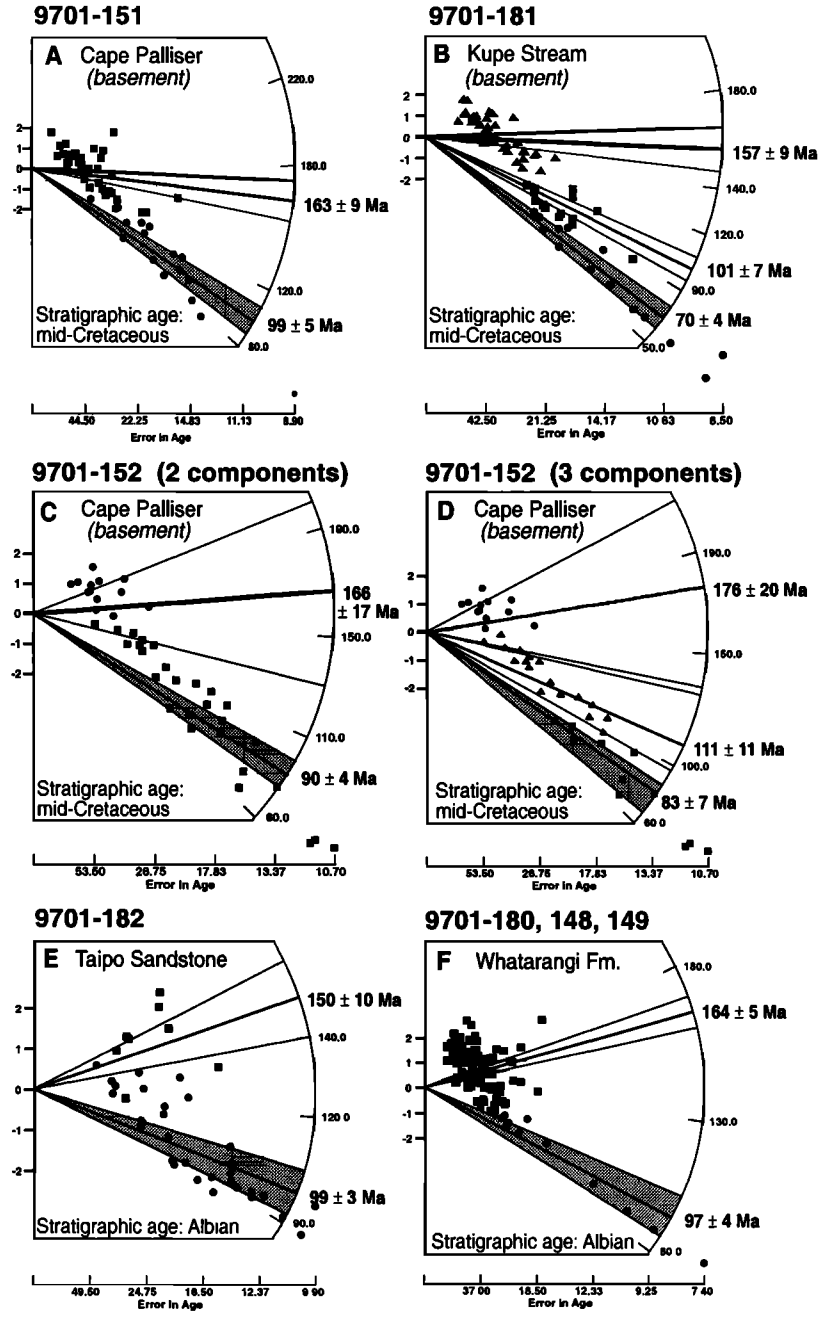

Figure 12. Radial plots for samples from the Waioeka Terrane (Omaio facies) and Whatarangi Formation in Aorangi Range, showing in particular the occurrence of the youngest age component, which for 9701-151, 9701-182 and 9701-180, 9701-148, 9701-149 are detrital and for 9701-152 and 9701–181 are partially thermally overprinted, reflecting heating from dike intrusions. Stratigraphic ages are based on current understanding and correlations to absolute timescales, which in some cases appear marginally too old.

conservative interpretation of two modes, the younger one being 99 ± 5 Ma, is adopted here. The importance of this young component is that it gives a maximum age on deposition and accretion of the host sandstone. Radiolarians in the adjacent colored argillite suggest an age no older than the start of the Coniacian Stage (89 Ma) (section 2.3)

Samples 9701-152 and 9701-181 come from localities within a few meters of undeformed lamprophyre dikes that intrude the basement succession. The field occurrence and petrography of these dikes have been described by *Challis* [1960]. The 67 grains dated in 9701-181 failed the chi-square test and are best described by three age components (Figure 12b). The young mode has an age of 70 ± 4 Ma, which cannot be viewed as having a detrital origin. It probably reflects resetting of zircon FT ages in the grains more susceptible to annealing by heating associated with intrusion of the dikes. The 70 ± 4 Ma age, is a maximum age, as the zircons with young ages may not have been completely annealed. Sample 9701-152 also failed the chi-square test. Radial plots with the component ages calculated with Fatmix software are shown in Figures 12c and 12d. The young mode is either 90 ± 4 (two components, Figure 12c) or 83 ± 7 Ma (three components; Figure 12d). The former could be a detrital

age component, but the latter (83 ± 7 Ma), preferred as the youngest mode, is interpreted as arising from partial resetting due to thermal affects associated with the dike intrusion at the sample locality.

Sample 9701-182 is from Taipo Sandstone, failed the chi-square test, and is described best by two age components (Figure 12e), one of 150 ± 10 Ma and another of 99 ± 3 Ma. Three-component analysis yielded ages of 99 ± 3, 99 ± 16, and 150 ± 11 Ma. The younger age component is consistent with the occurrence of redeposited Albian macrofossils and is the same age as identified in the highly indurated basement at Cape Palliser (9701-151).

Zircon FT ages are reported for three samples (9701-148, 9701-149 and 9701–181) from the Whatarangi Formation, which have similar sample mean FT ages in the range 156–167 Ma (Table 3). A radial plot incorporating the individual grain ages from all three samples shows a wide range of ages and, in particular, a young component of crystals with an age of 97 ± 4 Ma (two components, Figure 12f), or 94 ± 5 Ma (three components). Either of these ages in the context of their errors would be compatible with the Albian age of macrofossil species identified in the deposits sampled [*Speden*, 1968]. The young zircon component will be of detrital origin and helps to constrain the maximum stratigraphic age of the deposit.

7. Discussion and Implications

7.1. Zircon FT Detrital Ages and Model of Subduction Accretion

A key observation of the zircon FT ages for the basement rocks in the Aorangi Range is that the Taipo Sandstone, Palliser succession, and Whatarangi Formation all appear to contain a component of grains with circa 100 Ma detrital FT ages. Taken together with fossil age constraints, this could imply more-or-less contemporaneous deposition and accretion of these units. How could this have been achieved?

Figure 13, modified from *Hirono and Ogawa* [1998], illustrates schematically a structural arrangement in a subduction prism at which sediments could be thickened simultaneously at shallow and deeper levels by underplating of underthrust sediments, by offscraping and understuffing at the toe of the prism, and by subduction kneading within the prism associated with displacement on out-of-sequence thrusts bounding accretionary slope basin fills. The highly indurated complexes at Cape Palliser could have formed by underplating of trench sediments, although *George* [1990] preferred accretion by offscraping at the toe of a prism. The low rank Mangapokia Group (including Taipo Sandstone), known to have been deformed by accretionary processes [*Barnes and Korsch*, 1990], would have been accreted by understuffing at high structural levels at the top of the contemporary prism. The Whatarangi Formation represents siliciclastic sediments in route to the trench but trapped on the slope in an accretionary basin. The zircon FT data imply a common provenance and the simultaneous deposition and accretion of sediments in different parts of the Cretaceous prism. This multistorey accretion is facilitated by the characteristic horizontal incorporation of material into subduction prisms driven by lithospheric plate convergence. The modern day juxtaposition of different parts of the subduction complex at the surface is explained by Neogene faulting that has juxtaposed the Whatarangi Formation and the Palliser complex and by the higher amounts of Miocene erosion in southern versus northern parts of the Aorangi Range, as indicated by the apatite FT data reported above.

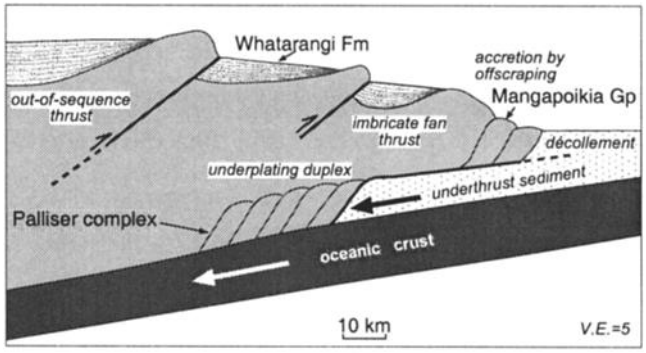

Figure 13. Schematic model of a subduction prism modified from *Hirono and Ogawa* [1998] showing the simultaneous multistorey incorporation of sediments into the prism by underplating, offscraping and out-of-sequence thrusting. This model may have applied during the mid-Cretaceous to the rocks now exposed in the Aorangi Range and helps to explain the same detrital FT age component (circa 100 Ma) in basement rocks of different levels of induration and rank.

7.2. Late Cretaceous (Circa 89–85 Ma) Termination of Subduction

Current debate centers on the timing within the Cretaceous of the termination of subduction (Pacific or Phoenix Plate) beneath New Zealand crust. The established argument [e.g., *Bradshaw*, 1989; *Laird*, 1992] has this occurring at about 105 Ma, immediately before the start of rifting in western South Island, which was followed by Tasman Sea spreading at about 80 Ma [*Weissel and Hayes*, 1997]. An alternative argument [*Mazengarb and Harris*, 1994] has the termination of subduction at about 85 Ma based on structural and stratigraphic evidence of an actively seaward migrating thrust system involving Cretaceous rocks in northeastern North Island (Raukumara Peninsula) and a change to deposition of a postsubduction passive margin succession. This later timing for the termination of subduction allows for concurrent rifting and subduction in the New Zealand region between circa 102 and circa 85 Ma.

For the rocks underlying the Aorangi Range, Figure 14 summarizes radiolarian age ranges and zircon FT detrital ages that help to constrain the timing of the termination of subduction in the region. Key radiolarian taxa in the Palliser complex are *Pseudodictyomitra lodagoensis* Pessagno (Albian-Cenomanian, 112.2–93.8 Ma) at Mangatoetoe Stream and *Stichomitra manifesta* sensu Taketani (Coniacian–Santonian, 89.0–83.0 Ma) [*Hashimoto and Ishida*, 1997] at Cape Palliser. While the age range of *P. lodagoensis* is well known, some uncertainty surrounds that of *S. manifesta* outside of Japan (C. Hollis, personal communication, 1998). Consequently, on the basis of their radiolarian content, the basement rocks at their oldest are Albian in age but could be as young as Santonian. As the deep ocean lithologic assemblages containing the radiolaria in the Palliser complex are allochthonous, the age ranges of the key taxa will give maximum ages on the timing of the subduction accretion that incorporated them into the prism and hence maximum ages on the termination of the subduction regime.

Figure 14 illustrates the 2σ age ranges of the youngest component of the detrital zircon FT ages from the basement complex and Whatarangi Formation. These age ranges also place

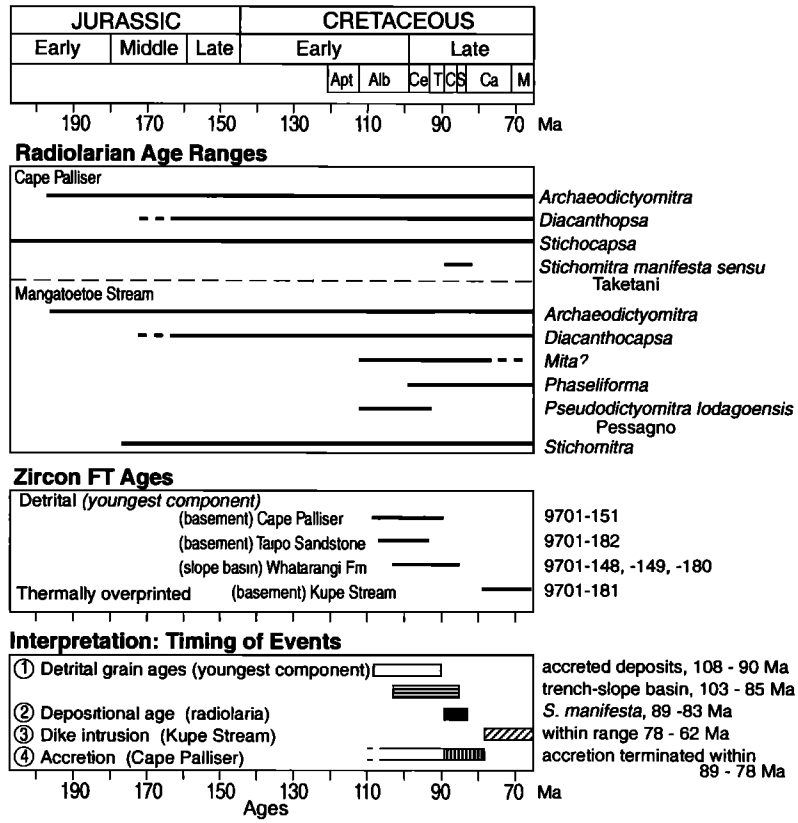

Figure 14. Compilation of age ranges for radiolaria identified [*George*, 1993; C. Hollis, personal communication, 1998] in Torlesse rocks at two localities (Cape Palliser and Mangatoetoe Stream) in Aorangi Range and the 2σ age range of the youngest component of detrital zircon fission track ages established for basement and slope basin deposits. Also shown is the 2σ age range of the youngest component of thermally overprinted zircon grains at the Kupe Stream locality resulting from dike intrusion. The radiolarian age ranges and zircon fission track ages are interpreted in terms of the termination of subduction accretion between 89 and 78 Ma. See text for discussion.

maximum ages on the timing of the termination of subduction accretion, which are Albian-Conacian (Cape Palliser) and Albian-Cenomanian (Taipo Sandstone). Slope basin deposition continued until at least Albian-Santonian.

Minimum ages on the termination of subduction may be provided by the component of zircon crystals reset by camptonitic postsubduction dike intrusions at Kupe Stream, which have a 2σ age range of 78–62 Ma. This is consistent with stratigraphic evidence for a major change in the style of sedimentation at circa 85 Ma (mid-Piripauan Stage) throughout eastern North Island [*Mazengarb and Harris*, 1994; *Field and Uruski*, 1997]. The maximum radiolarian and detrital zircon FT ages obtained, together with the minimum FT ages on dike intrusion, constrain the termination of subduction accretion in the Aorangi-Palliser area to lie within 89–78 Ma (Figure 14), and more probably 89–85 Ma, taking account of the eastern North Island cover stratigraphy. The older age limit is critically dependent on the age of the first appearance in the southwest Pacific of *S. manifesta*; if this is shown to predate the Coniacian, the older age constraint on the timing of the termination of subduction will become correspondingly older. The significance of the interpretation made here that subduction may have terminated as late as 89–85 Ma in southern North Island is that it shows that the Raukumara Peninsula record of a circa 85 Ma termination of subduction [*Mazengarb and Harris*, 1994; *Kamp*, 1999] is not an exception or special case that only applies to that area. Rather, a late Cretaceous timing for the termination of subduction applies to the whole of the eastern North Island part of the paleomargin.

7.3. Age and Distribution of Terranes Within the Torlesse Complex, North Island

The detrital zircon FT and radiolarian ages summarized in section 7.2 (Figure 14) indicate that basement rocks in the Aorangi Range may be as young as early-Late Cretaceous. Although previously included in the Pahau Terrane, their deposition and accretion were clearly later than that for Pahau sequences in the axial ranges of North Island (*Mortimer's* [1995] Late Jurassic-Early Cretaceous axial B rocks). Moreover, the Aorangi Range basement has the same circa 100 Ma detrital zircon FT ages as the Omaio Facies of the Waioeka Terrane in Raukumara Peninsula [*Kamp*, 1999; *Cawood et al.*, 1999]. For Raukumara Peninsula, *Mortimer* [1995] included the Omaio petrofacies within his Waioeka (sub)terrane but also noted that the same feldsarenite facies (known to be of older age) occurs within Pahau Terrane (axial B) as well. What emerges from the new data presented and interpreted in this paper is further age and geographic differentiation within the younger Torlesse sequences (Pahau and Waioeka Terranes) of eastern North Island. Figure 15 maps the Aorangi Range basement with circa 100 Ma detrital zircons and surrounding sequences of similar structural character [*Moore and Speden*, 1984] as part of an Omaio belt within

Waioeka Terrane. The unity of this belt throughout eastern North Island needs to be confirmed with further zircon dating and the identification of circa 100 Ma detrital ages. The outcrop pattern that seems to emerge for the younger Torlesse is one with two parallel terranes (Pahau and Waioeka) with the Waioeka Terrane comprising two belts, one comprising litharenites and the other feldsarenites (Omaio belt) in a more outboard position (Figure 15). It is tempting to think of these three belts (Pahau (axial B), Waioeka litharenites, Omaio feldsarenites) as having been successively deposited and accreted to the paleosubduction margin through the Late Jurassic–Late Cretaceous. This seems to be supported by the detrital zircon FT age distributions established for each of these three belts so far (Table 3) [*Kamp*, 1999, Table 1 and Figure 4], in which the youngest age component gets younger across the margin to the east. As noted above, further work needs to be done to confirm these indications. It is also worth noting that the extent of the Omaio belt emphasizes the volume of sediments delivered to the margin from terrigenous sources during the Early to early Late Cretaceous, which in turn probably reflects major denudation in the contemporary continental margin hinterland. This would seem to postdate a circa 120-130 Ma phase of magmatism reflected in the detrital zircon FT ages [*Kamp*, 1999] in the litharenites of the Waioeka Terrane.

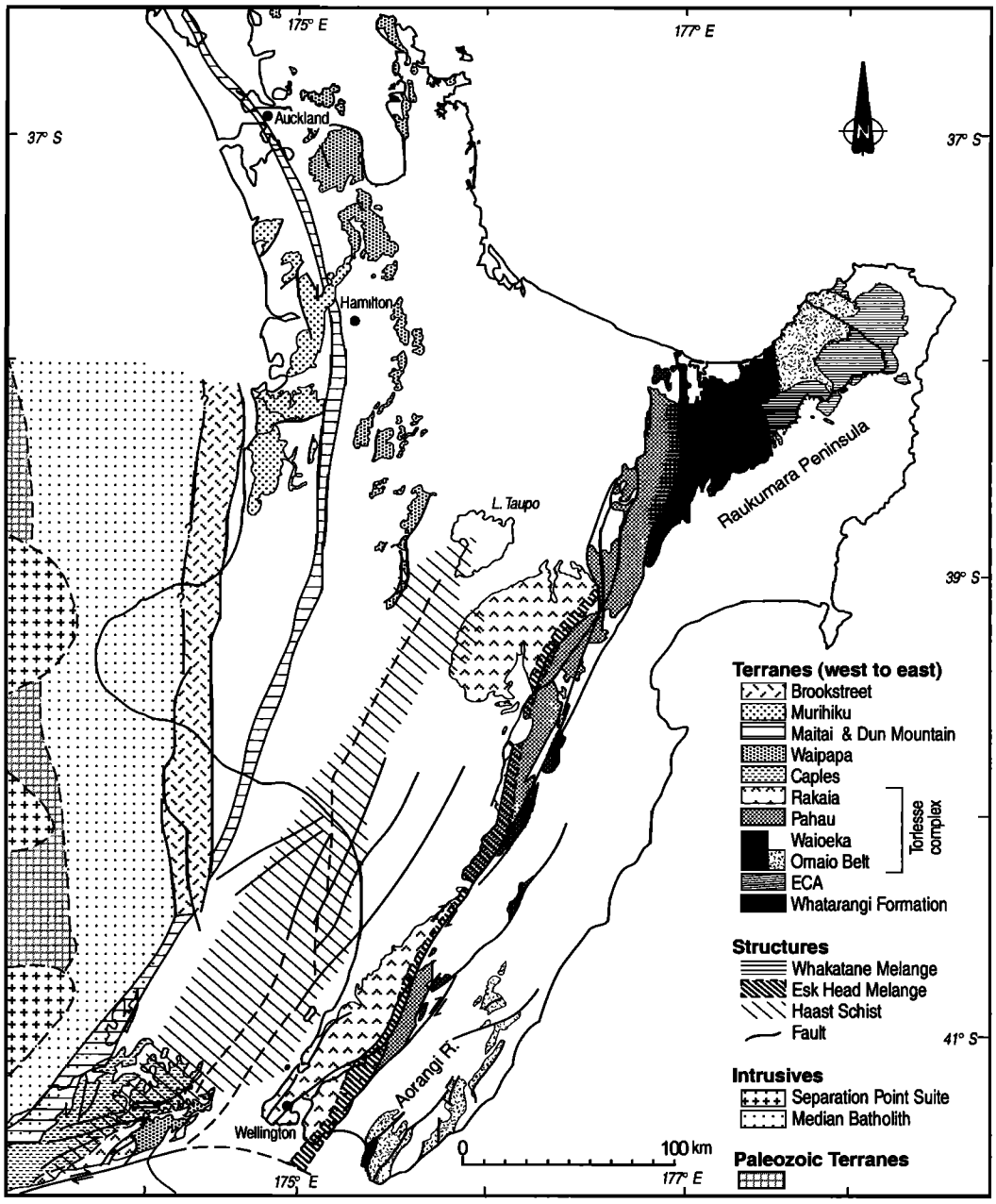

Figure 15. Map of North Island showing the distribution of basement terranes, in particular those in the Torlesse Complex, based on works by *Spörli* [1978], *Mortimer* [1993, 1995], and *Mortimer et al.* [1997], modified to show Omaio belt in the Aorangi Range, as discussed in the text. This change emphasizes the extent of the Waioeka Terrane, being the youngest of the Mesozoic accretionary complexes in North Island.

7.4. Distribution and Timing of Exhumation Across the Torlesse Accretionary Complexes

The exhumation of the Torlesse accretionary complexes occurred partly during the Cretaceous for the older complexes and during the Neogene for all complexes. The apatite FT data reported above constrain the minimum amounts of cooling/exhumation during the Neogene as having been ~110°C (~4 km) across the whole of the southern transect. Northward along the Aorangi Range, however, the total amount of cooling/exhumation decreased to 68°C/~2.3 km at sample site 9801-182 (Figure 3). There may not have been much, if any, exhumation of the Palliser complex during the Late Cretaceous. Zircon FT ages in the Palliser complex are not partially annealed in situ and therefore are unlikely to have been heated in the prism to levels higher than ~210°C, at which partial annealing starts for timescales of heating of 10^7 to 10^8 years [*Tagami et al.*, 1996, 1998]. The zircon FT and $^{40}Ar/^{39}Ar$ ages for the Rakaia Terrane (Wellington Belt) indicate 265–310°C of cooling. A maximum of 155–200°C (~6–8 km) of this cooling could have occurred during the Cretaceous (for total Neogene cooling of 110°C). This implies substantial uplift and erosion of inboard parts of the Torlesse Complex contemporaneously with accretion of the Palliser complex.

The thermochronological data and their interpretations, together with the present-day structural arrangement (Figure 2), give some insights into how the Torlesse Complex may have been tectonically amalgamated and exhumed. The Neogene exhumation and rock uplift have clearly been driven by interactions of the Australian and Pacific Plates across the subduction thrust and are associated with the underplating and accretion of a prism beneath the modern shelf and slope and outboard of the Palliser complex. That underplating and accretion has exhumed the Palliser complex during the Neogene in the Aorangi Range, in association with a strike-slip regime driven by the oblique subduction. This may be an analogue for Cretaceous exhumation of the inner parts (Rakaia to Pahau Terranes) of the Torlesse Complex. It is envisaged that Cretaceous underthrusting of the Palliser complex rotated counterclockwise with thrusting and shortening the Rakaia-Pahau Terranes, causing their exhumation. This resulted in substantial foreshortening of the width of the original prism. Moreover, this model of exhumation implies that the base of one accretionary prism is juxtaposed with the top of another. A corollory is that the terrane (prism) boundaries, which in the Torlesse Complex are melange zones (Esk Head Melange, Whakatane Melange, Figure 15), represent parts of fossil subduction thrusts.

7.5. (Re-)Interpretation of Whole Rock K-Ar and Rb-Sr Age Data for the Wellington Area

Extensive whole rock K-Ar and Rb-Sr dating has been undertaken previously on Torlesse rocks in the Wellington-Palliser area [*Adams and Graham*, 1993, 1996; *George and Graham*, 1991; *Graham and Adams*, 1990; *Graham and Korsch*, 1989], and a particular geological history has been interpreted from these data by their authors. The derivation of zircon fission track ages (a different thermochronological system but with a similar paleotemperature range) for the same rock succession gives an opportunity to evaluate the extensive K-Ar and Rb-Sr whole rock data set and what the ages mean geologically and the uniqueness of the derived geological history as published. The K-Ar and Rb-Sr data and their interpretation are comprehensively summarized by *Adams and Graham* [1996]. More recently, there has been a move to $^{40}Ar/^{39}Ar$ dating of muscovite and biotite concentrates from the rocks [*Adams and Kelley*, 1998], but elements of the geological history (timing of regional metamorphism, imbrication, and formation of schistose fabrics) inferred from the whole rock ages persist [e.g., *Adams and Kelley*, 1998; *Adams et al.*, 1998].

In the Wellington Belt of the Rakaia Terrane the whole rock K-Ar data show a wide scatter, with ages on different localities ranging between 223 ± 3 and 102 ± 1 Ma [*Adams and Graham*, 1996]. Only 5% of the ages are less than 130 Ma and all but two of the samples in this group originate from one locality (Cape Terawhiti), where, within a few hundred metres, the sample ages range between 183 ± 2 and 102 ± 1 Ma. Most of the sample ages are less than the corresponding stratigraphic ages based on fossil content, and the samples with younger ages are within shear zones or zones of semischist. These age data have been interpreted [e.g., *Adams and Graham*, 1996] to indicate complete argon degassing by burial metamorphism during the latest Triassic to earliest Jurassic, leading up to peak metamorphism at 200–190 Ma, followed by postmetamorphic uplift and cooling through to middle Jurassic (circa 170 Ma). This was followed by Early Cretaceous thermal overprinting in narrow zones of semischists associated with imbrication of the younger Torlesse.

The pattern in the zircon FT data for the same rocks implies a different interpretation: that all of the whole-rock K-Ar ages except those few percent less than about 130 Ma are part of an argon partial retention zone [*Kamp et al.*, 1989] fossilized through uplift and erosion at about 130 Ma. This argon partial retention zone shows the same characteristics as the zircon FT partial annealing zone described in section 5.1. The measured K-Ar ages are mostly less than the stratigraphic age range of the Wellington Belt, with only the youngest ages having been totally degassed or near to total degassing, prior to the start of an Early Cretaceous cooling phase. At all localities sampled, with some results coming from different lithologic fractions in adjacent beds, the ages vary markedly, just as individual zircon crystals from a bed which has resided within a partial annealing zone can show a wide spread in single grain ages, reflecting different retentive properties with respect to the radiogenic daughter product. The interpretation that all of the rocks were totally degassed of argon during some metamorphic peak in the earliest Jurassic [e.g. *Adams and Graham*, 1996] does not fit with the individual crystal $^{40}Ar/^{39}Ar$ ages reported for the same rocks [*Adams and Kelley*, 1998] (Figure 10) in which the muscovites possibly show small degrees of partial argon degassing and some of the biotite crystals are reset. The paleotemperature modeling undertaken of the three thermochronological systems ($^{40}Ar/^{39}Ar$ and FT ages) for which we currently have data (section 5.3, Figure 11) can adequately explain the whole rock K-Ar data in terms of rapid burial and imbrication (225-200 Ma) with stable conditions until about 135 Ma when the rocks first cooled substantially. The whole rock K-Ar data fit this geological history. The lack of understanding of the kinetics of radiogenic argon retention in whole rocks of graywacke and semischist lithology at any timescale clearly precludes quantitative modeling from being undertaken and makes even qualitative interpretation of such data difficult without reference to well-established thermochronometers. The whole rock K-Ar ages reported for basement from the Aorangi Range range between 144 ± 2 and 39 ± 1 Ma. By reference to the zircon FT data reported here, these K-Ar ages older than circa 100 Ma are possibly provenance ages. The K-Ar ages less than circa 100 Ma may have been partially to totally overprinted by the late Cretaceous phase of dike intrusion associated with the regional recovery of geothermal gradients

following the termination of Mesozoic subduction in the New Zealand region [*Kamp and Liddell*, 2000].

The whole rock Rb-Sr data reported for rocks from the Wellington Belt, as for the K-Ar data, have been interpreted in terms of having undergone complete strontium isotopic homogenization during prograde metamorphism and isochron ages interpreted to date progressive late Triassic-earliest Jurassic (225–170 Ma) eastward imbrication of the Rakaia accretionary prism [e.g., *Adams and Graham*, 1996]. Younger (Middle Jurassic-Early Cretaceous) Rb-Sr isochron ages associated with shear zones and semischists are interpreted as representing a separate partial to total homogenization event. We interpret all these data more simply in terms of one partially homogenized Rb-Sr zone fossilized during the Early Cretaceous by uplift, faulting, and erosion. An important observation, as for the whole rock K-Ar ages, is that the youngest isochron ages are associated with the highest-grade rocks [*Adams and Graham*, 1993, 1996], representing the deepest structural levels now exposed at the surface. It follows from the new interpretation that the notion of a latest Triassic-earliest Jurassic peak metamorphic event needs to be abandoned. Moreover, the practice of always interpreting linear arrays of Rb-Sr data points for sedimentary rocks as isochrons that have meaning in terms of geological events needs to be reconsidered. There is a need to better understand the systematics of the Rb-Sr system during burial/diagenesis/prograde metamorphism to establish conditions under which Sr homogenization is complete and criteria to judge when this has occurred. To this end it may be useful to analyze mineral, matrix, and cement phases within rocks.

Rb-Sr isochron ages (136 ± 3 to 145 ± 8 Ma) for basement from the Aorangi Range have been interpreted as true metamorphic ages [*Adams and Graham*, 1996]. This interpretation conflicts with the circa 100 Ma depositional age of some of these rocks based on the zircon FT data presented above. The Rb-Sr isochron age of 72 ± 2 Ma on a hyaloclastite within the metavolcanic sediments of Cape Palliser is within error of the age of 70 ± 4 Ma obtained here for the dike intrusions and may well be a rock that was completely reset due to it having a particular composition that made it more susceptible to isotopic resetting [*Adams and Graham*, 1996]. The Rb-Sr isochron ages of 90 ± 13± Ma at Cape Palliser (metavolcanics) and 81 ± 6 Ma (turbidite, Cod Rocks) are interpreted as being partially reset due to the thermal effects of dike intrusion.

Acknowledgments. Valuable assistance with field sampling was provided by Xu Ganqing and technical assistance in the fission track laboratory by Ivan Liddell and Xu Ganqing. Six of the samples were also kindly provided by Hamish Campbell and John Begg. I am very grateful to Chris Hollis for reviewing the identification and age ranges of radiolarians reported previously from Kupe Stream and Cape Palliser. Reviews by N. Mortimer, T. Tagami, G. Rait, and Associate Editor James Brenan were helpful in revising the manuscript and are appreciated. I am also grateful to Elaine Norton for word-processing the manuscript and to Betty-Ann Kamp for the cartographics.

References

Adams, C.J., and I.J. Graham, K-Ar and Rb-Sr age studies of the metamorphism and quartz vein Au mineralisation on Terawhiti Hill, near Wellington, New Zealand, *Chem. Geol., 103*, 235-249, 1993.

Adams, C.J., and I.J. Graham, Metamorphic and tectonic geochronology of the Torlesse Terrane, Wellington, New Zealand, *N. Z. J. Geol. Geophys., 39*, 157-180, 1996.

Adams, C.J., and S. Kelley, Provenance of Permian-Triassic and Ordovician metagreywacke terranes in New Zealand: Evidence from $^{40}Ar/^{30}Ar$ dating of detrital micas, *Geol. Soc. Am. Bull., 110*, 422-432, 1998.

Adams, C.J., M.E. Barley, I.R. Fletcher, and A.L. Pichard, Evidence from U-Pb zircon and $^{40}Ar/^{39}Ar$ muscovite detrital mineral ages in metasandstones for movement of the Torlesse suspect terrane around the eastern margin of Gondwanaland, *Terra Nova, 10*, 183-189, 1998.

Andrews, P.B., I.G. Speden, and J.D. Bradshaw, Lithological and palaeontological content of the Carboniferous-Jurassic Canterbury Suite, South Island, New Zealand, *N. Z. J. Geol. Geophys., 19*, 791-819, 1976.

Baldwin, S.L., and G.S. Lister, Thermochronology of the South Cyclades Shear Zone, Ios, Greece: Effects of ductile shear in the argon partial retention zone, *J. Geophys. Res., 103*, 7315-7336, 1998.

Barnes, P.M., and R.J. Korsch, Structural analysis of a middle Cretaceous accretionary wedge, Wairarapa, New Zealand, *N. Z. J. Geol. Geophys., 33*, 355-375, 1990.

Barnes, P.M., and R. J. Korsch, Melange and related structures in Torlesse accretionary wedge, Wairarapa, New Zealand, *N. Z. J. Geol. Geophys., 34*, 517-532, 1991.

Barnes, P.M., B. Mercier de Lépinay, J-Y. Collot., J. Delteil, and J.-C. Audru, Strain partitioning in the transition area between oblique subduction and continental collision, Hikurangi margin, New Zealand, *Tectonics, 17*, 534-557, 1998.

Begg, J.G., and C. Mazengarb, Geology of the Wellington area, *Geol. Map 22*, 1 sheet + 128 pp., Inst. of Geol. and Nucl. Sci., Lower Hutt, New Zealand, 1996.

Blome, C.D., P.R. Moore, J.E. Simes, and W.A. Watters, Late Triassic radiolaria from phosphatic concretions in the Torlesse terrane, Kapiti Island, Wellington. *N. Z. Geol. Surv. Rec., 18*, 103-109, 1987.

Bradshaw, J.D., Cretaceous geotectonic patterns in the New Zealand region, *Tectonics, 8*, 803-820, 1989.

Bradshaw, J.D., P.B. Andrews, and C.J.D Adams, Carboniferous to Cretaceous on the Pacific margin of Gondwana: The Rangitata phase of New Zealand, in *Gondwana 5*, edited by M.M. Cresswell and P. Vella, pp. 217-221, A.A. Balkema, Brookfield, Vt., 1981.

Brandon, M.T., M.R. Roden-Tice, and J.I. Garver, Late Cenozoic exhumation of the Cascadia accretionary wedge in the Olympic Mountains, northwest Washington State, *Geol. Soc. Am. Bull., 110*, 985-1009, 1998.

Campbell, H.J., *Halobia* (Bivalvia, Triassic) and a gastropod from Torlesse Supergroup rocks of Wellington, New Zealand, *N. Z. J. Geol. Geophys., 25*, 487-492, 1982.

Cawood, P.A., A.A. Nemchin, A. Leverenz, A. Saeed, and P. Ballance, U/Pb dating of detrital zircons: Implications for the provenance record of Gondwana margin terranes, *Geol. Soc. Am. Bull., 111*, 1107-1119, 1999.

Challis, G.A., Igneous rocks in the Cape Palliser area, *N. Z. J. Geol. Geophys., 3*, 524-542, 1960.

Coombs, D.S., C.A. Landis, R. Norris, R.M. Carter, D. Borns, and D. Craw, The Dum Mountain ophiolite belt, New Zealand, its tectonic setting, constitution, and origin, with special reference to the southern portion, *Am. J. Sci., 26*, 561-603, 1976.

Davey, F.J., M. Hampton, J. Childs, M.A. Fisher, K.B. Lewis, and J.R. Pettinga, Structure of a growing accretionary prism, Hikurangi margin, New Zealand, *Geology, 14*, 663-666, 1986.

Field, B.D., and C.I. Uruski, *Cretaceous-Cenozoic Geology and Petroleum Systems of the East Coast Region, New Zealand, Monogr. 19*, 301 pp., Inst. of Geol. and Nucl. Sci., Lower Hutt, New Zealand, 1997.

Fleischer, R.L., P.B. Price and R.M. Walker, *Nuclear Tracks in Solids*, 605 pp., Univ. of Calif. Press, Berkeley, 1975.

Foley, L.A., T.O.H. Orr, and R.J. Korsch, Radiolaria of Middle Jurassic to Early Cretaceous ages from the Torlesse Complex, eastern Tararua Ranges, New Zealand, *N. Z. J. Geol. Geophys., 29*, 481-490, 1986

Galbraith, R.F., On statistical methods of fission track counts, *Math. Geol., 13*, 471-478, 1981.

Galbraith, R.F., and P.F. Green, Estimating the component ages in a finite mixture, *Nucl. Tracks Radiat. Meas., 17*, 197-206, 1991.

Gallagher, K., Evolving temperature histories from apatite fission-track data, *Earth Planet. Sci. Lett., 136*, 421-435, 1995.

Gallagher, K., R. Brown, and C. Johnston, Fission track analysis and its applications to geological problems, *Annu. Rev. Earth Planet. Sci., 26*, 519-572, 1998.

Garver, J.I., and M.T. Brandon, Fission track ages of detrital zircon from mid-Cretaceous sediments of the Methow-Tyaughton Basin, southern Canadian Cordillera, *Tectonics, 13*, 401-420, 1994.

Garver, J.I., M.T. Brandon, M. Roden-Tice, and P.J.J. Kamp, Exhumation history of orogenic highlands determined by detrital fission track thermochronology, in *Exhumation Processes: Normal Faulting, Ductile Flow and Erosion*, edited by U. Ring et al, *Geol. Soc. Spec. Publ., 154*, 283-304, 1999.

George, A.D., Deformation processes in an accretionary prism: A study from the Torlesse terrane of New Zealand, *J. Struct. Geol., 12*, 747-759, 1990.

George, A.D., Deposition and deformation of an Early Cretaceous trench-slope basin deposit, Torlesse Terrane, New Zealand, *Geol. Soc. Am. Bull., 104*, 570-580, 1992.

George, A.D., Radiolarians in offscraped seamount fragments, Aorangi Range, New Zealand, *N. Z. J. Geol. Geophys., 36*, 185-199, 1993.

George, A.D., and I.J. Graham, Whole-rock Rb-Sr isochrons and pseudo-isochrons from turbidite suites from the Torlesse accretionary prism, New Zealand, *Chem. Geol., 87*, 11-20, 1991.

Gleadow, A.J.W., Fission track dating methods: what are the real alternatives?, *Nucl. Tracks Radiat. Meas., 5*, 15-25, 1981.

Gleadow, A.J.W., and P.F. Fitzgerald, Uplift history and structure of the Transantarctic Mountains: New evidence from fission track dating of basement apatites in the Dry Valleys area, southern Victoria Land, *Earth Planet. Sci. Lett., 82*, 1-14, 1986.

Gleadow, A.J.W., I.R Duddy, P.F. Green, and K A. Hegarty, Fission track lengths in the apatite annealing zone and the interpretation of mixed ages, *Earth Planet. Sci. Lett., 78*, 245-254, 1986.

Gradstein, F.M., F.P. Agterberg, J.G. Ogg, J. Hardenbol, P. van Veen, J. Thierry, and Z. Huang, A Mesozoic timescale, *J. Geophys. Res., 99*, 24,051-24,074, 1994

Graham, I.J., and C.J. Adams, Rb-Sr and K-Ar geochronology of turbidites and metavolcanics at Red Rocks, Wellington, New Zealand, *N. Z. J. Geol. Geophys., 33*, 193-200, 1990.

Graham, I.J., and R.J. Korsch, Rb-Sr resetting age and chemical characterisation of turbidites in an accretionary wedge: Torlesse Complex, Otaki Gorge, New Zealand. *Geol. Soc. Am. Bull., 101*, 355-363, 1989.

Grapes, R H., and H.J. Campbell, Red Rocks: A Wellington geological excursion, *Geol. Soc N. Z. guide. 11*, 32 pp., 1994.

Grapes, R.H., S.H. Lamb, H.J. Campbell, K.B. Spörli, and J.E. Simes, Geology of the Red Rocks–turbidite association, Wellington peninsula, New Zealand, *N. Z. J. Geol. Geophys., 33*, 377-391, 1990.

Green, P.F., Comparison of zeta calibration baselines for fission track dating of apatite, zircon and sphene, *Chem Geol., 58*, 1-22, 1985.

Green, P.F., I.R. Duddy, A.J.W. Gleadow, P.R. Tingate, and G.M. Laslett, Thermal annealing of fission tracks in apatite, 1, A qualitative description, *Chem. Geol., 59*, 237-253, 1986.

Green, P.F., I.R. Duddy, G.M. Laslett, K. Hegarty, A.J.W. Gleadow, and J.F. Lovering, Thermal annealing of fission tracks in apatite, 4; Quantitative modelling techniques and extensions to geological timescales, *Chem. Geol., 79*, 155-182, 1989

Hashimoto, H., and K. Ishida, Correlation of selected radiolarian assemblages of the Upper Cretaceous Izumi and Sotoizumi Groups and Shimanto Supergroup, in Shikoku, *News Osako Micropaleontol., Spec. Vol., 10*, 245-257, 1997.

Hirono, T., and Y. Ogawa, Duplex arrays and thickening of accretionary prisms: An example from Boso Peninsula, Japan, *Geology, 26*, 779-782, 1998.

Hurford, A.J., Cooling and uplift patterns in the Lepontine Alps, south central Switzerland, and an age of vertical movement on the Insubric fault line, *Contrib. Mineral. Petrol., 92*, 413-427, 1986.

Hurford, A.J., and P.F. Green, A guide to fission track dating calibration, *Earth Planet. Sci. Lett., 59*, 343-354, 1982.

Hurford, A.J., F.J. Fitch, and A. Clarke, Resolution of the age structure of the detrital populations of two lower Cretaceous sandstones from the Weald of England by fission track dating, *Geol. Mag., 121*, 269-277, 1984.

Kamp, P.J.J., Tracking crustal processes by FT thermochronology in a forearc high (Hikurangi Margin, New Zealand) involving Cretaceous subduction termination and mid-Cenozoic subduction initiation, *Tectonophysics, 307*, 313-343, 1999.

Kamp, P.J.J., and I. Liddell, Thermochronology of northern Murihiku Terrane, New Zealand, derived from apatite FT analysis, *J Geol Soc. London, 155*, 345-354, 2000.

Kamp, P.J.J., P.F. Green, and S.H. White, Fission track analysis reveals character of collisional tectonics in New Zealand, *Tectonics, 8*, 169-195, 1989.

Laird, M.G., Cretaceous stratigraphy and evolution of the Marlborough segment of the East Coast region, in *Proceedings of New Zealand Oil Exploration Conference, 1991*, pp. 89-100, Minist. of Commer., Wellington, 1992.

Laslett, G.M., W.S. Kendall, A.J.W Gleadow, and I.R. Duddy, Bias in the measurement of fission track length distributions, *Nucl. Tracks, 6*, 79-85, 1982.

Lister, G.S., and S.L. Baldwin, Modelling the effect of arbitrary P-T-t histories on argon diffusion in minerals using the MacArgon program for the Apple Macintosh, *Tectonophysics, 253*, 83-109, 1996.

MacKinnon, T.C., Origin of the Torlesse terrane and coeval rocks, South Island, New Zealand, *Geol Soc. Am. Bull., 94*, 967-985, 1983.

Mazengarb, C., and D H.M. Harris, Cretaceous stratigraphic and structural relations of Raukumara Peninsula, New Zealand: Stratigraphic patterns associated with the migration of a thrust system, *Ann. Tectonica, VIII*, 100-118, 1994.

Moore, P.R., and I.G. Speden, The Early Cretaceous (Albian) sequence of eastern Wairarapa, New Zealand, *N. Z. Geol. Surv. Bull., 97*, 98pp., 1984.

Mortimer, N., Metamorphic zones, terranes and Cenozoic faults in the Marlborough Schist, New Zealand, *N. Z. J. Geol. Geophys., 36*, 357-368, 1993.

Mortimer, N., Origin of the Torlesse Terrane and coeval rocks, North Island, New Zealand, *Int. Geol. Rev., 36*, 891-910, 1995.

Mortimer, N., H.C. McIntyre, and D.H.M. Harris, Terawhiti Schist, *Geol. Soc. N Z. Misc. Publ., 79B*, 45-63, 1993.

Mortimer, N., A.J. Tulloch, and T.R. Ireland, Basement geology of Taranaki and Wanganui Basins, New Zealand, *N. Z J. Geol. Geophys., 40*, 223-236, 1997.

Reed, J.J., Petrology of the lower Mesozoic rocks of the Wellington District, *N. Z. Geol. Surv. Bull., 57*, 1957.

Robinson, R., Seismicity within a zone of plate convergence–the Wellington region, New Zealand, *Geophys. J. R. Astron. Soc., 55*, 693-702, 1978.

Robinson, R., Seismicity, structure and tectonics of the Wellington Region, New Zealand, *Geophysics J. R. Astron. Soc., 87*, 379-410, 1986.

Roser, B., R. Grapes, and K. Palmer, Geochemistry and distribution of greywacke turbidites, coloured siltstones, carbonate and phosphorite: in *Geology of the Wellington Area*, by J. Begg, and C. Mazengarb, Inst. of Geol. and Nucl. Sci. *Geol. Map 22*, pp. 117-120, Lower Hutt, New Zealand, 1996.

Sambridge, M.J., and W. Compston, Mixture modelling of multi-component data sets with application to ion-probe zircon ages, *Earth Planet. Sci. Lett., 128*, 373-390, 1994.

Silberling, N J., K.M. Nichols, J D Bradshaw, and C D. Blome, Limestone and chert in tectonic blocks from the Esk Head subterrane, South Island, New Zealand, *Geol. Soc. Am Bull., 100*, 1213-1223, 1988.

Speden, I.G., Lower Cretaceous marine fossils, including *Maccoyella* sp., from the Whatarangi Formation, east side of Palliser Bay, New Zealand, *Trans. R. Soc. N. Z., 6*, 143-153, 1968.

Speden, I.G., Fossil localities in Torlesse rocks of the North Island, New Zealand, *J. R Soc. N. Z., 6*, 73-91, 1976

Spörli, K.B., Mesozoic tectonics, North Island, New Zealand, *Geol. Soc. Am. Bull., 89*, 415-425, 1978

Stock, J., and P. Molnar, Uncertainties in the relative positions of the Australia, Antarctica, Lord Howe and Pacific plates since the Late Cretaceous, *J. Geophys Res., 87*, 4679-4714, 1982.

Suggate, R P., G.R. Stevens, and M.T. Te Punga, *The Geology of New Zealand, Vol. 1*, N Z. Geol. Surv., Dep. of Sci and Ind Res., Govt. Print., Wellington, 1978.

Suneson, N.H., The geology of the Torlesse Complex along the Wellington area coast, North Island, New Zealand, *N. Z. J. Geol Geophys., 36*, 369-384, 1993.

Tagami, T., A. Carter, and A.J. Hurford, Natural long-term annealing of the zircon fission-track system in Vienna Basin deep borehole samples: Constraints upon the partial annealing zone and closure temperature, *Chem. Geol., 130*, 147-157, 1996.

Tagami, T., R.F. Galbraith, R Yamada, and G.M. Laslett, Revised annealing kinetics of fission tracks in zircon and geological implications, in *Advances in Fission-Track Geochronology*, edited by P. Van den Haute and F. de Corte, pp. 99-112, Kluwer Acad., Norwell, Mass., 1998.

Walcott, R.I., Present tectonics and Late Cenozoic evolution of New Zealand, *Geophys. J. R. Astron. Soc., 83*, 4419-4429, 1978.

Weissel, J K., and D.E. Hayes, Evolution of the Tasman Sea reappraised, *Earth Planet. Sci. Lett., 36*, 77-84, 1977.

P.J.J. Kamp, Department of Earth Sciences, University of Waikato, Private Bag 3105, Hamilton, New Zealand. (p.kamp@waikato.ac.nz)

(Received July 9, 1999; revised January 20, 2000;
accepted March 20, 2000.)